Heliyon 6 (2020) e05743

Contents lists available at ScienceDirect

Heliyon

journal homepage: www.cell.com/heliyon

Research article

Antioxidative attributes of rice bran extracts in ameliorative effects of atherosclerosis-associated risk factors

Xian Wen Tan [a], Kazuko Kobayashi [b], Lianhua Shen [c], Junko Inagaki [a], Masahiro Ide [a,d], Siaw San Hwang [e], Eiji Matsuura [a,b,f,*]

[a] Department of Cell Chemistry, Okayama University Graduate School of Medicine, Dentistry, and Pharmaceutical Sciences, Okayama, Japan
[b] Collaborative Research Center for OMIC, Okayama University Graduate School of Medicine, Dentistry, and Pharmaceutical Sciences, Okayama, Japan
[c] Department of Pathophysiology, Zunyi Medical University, Guizhou, China
[d] Food Function Research Team, Saito Laboratories, Japan Food Research Laboratories, Osaka, Japan
[e] School of Chemical Engineering and Science, Faculty of Engineering, Computing and Science, Swinburne University of Technology Sarawak Campus, Sarawak, Malaysia
[f] Neutron Therapy Research Center, Okayama University, Okayama, Japan

ARTICLE INFO

Keywords:
Food science
Food analysis
Rice bran extract (RBE)
Functional food
Phytochemicals
Atherosclerosis
Oxidative stress
Inflammation
Antioxidant
Anti-inflammation
Oxidized lipoprotein (oxLDL)

ABSTRACT

Oxidative stress, chronic inflammation, dyslipidemia, hyperglycemia, and shear stress (physical effect) are risk factors associated with the pathogenesis of atherosclerosis. Rice bran, a by-product of rice milling process, is known to house polyphenols and vitamins which exhibit potent antioxidant and anti-inflammatory properties. Through recent emerging knowledge of rice bran in health and wellness, the present study was aimed to assess the ameliorative effects of rice bran extracts (RBE) derived from Japanese colored rice varieties in modulating risk factors of atherosclerosis via *in vitro* and *in vivo* study models. Pre-treatment of lipopolysaccharide (LPS)-stimulated murine J774A.1 macrophage-like cells with RBE alleviated nitric oxide (NO) overproduction and down-regulated gene expressions of pro-inflammatory modulators: tumor necrosis factor-α (TNF-α), interleukin (IL)-α (IL-1α), IL-1β, IL-6, and inducible nitric oxide synthase (iNOS). In addition, RBE also significantly attenuated LPS-stimulated protein expressions of iNOS, TNF-α, IL-1α, and IL-6 in J774A.1 macrophage-like cells as compared to non-treated LPS control group. In *in vivo*, 12 weeks of RBE dietary supplementations significantly reduced ($p < 0.05$) total cholesterol, triglycerides, and pro-atherogenic oxidized LDL/β2-glycoprotein I (oxLDL/β2GPI) complexes at plasma levels, in high fat diet (HFD) induced low density lipoprotein receptor knockout ($Ldlr^{-/-}$) mice. En face pathological assessments of murine aortas also revealed significant reductions by 38% ($p < 0.05$) in plaque sizes of RBE-supplemented HFD mice groups as compared to non RBE-supplemented HFD control mice group. Moreover, gene expressions of aortic (iNOS, TNF-α, IL-1β) and hepatic (TNF-α, IL-1α, IL-1β) pro-inflammatory modulators were also downregulated in RBE-supplemented mice groups. Present study has revealed the potent health attributes and application of RBE as a dietary supplement to attenuate risks of inadvertent oxidative damage and chronic inflammation underlying the pathogenesis of atherosclerosis. Intrinsically, present preliminary findings may provide global health prospects for future dietary implementation of RBE in management of atherosclerosis.

1. Introduction

Atherosclerosis, the hardening of arteries, is one of the prevalent forms of cardiovascular disease (CVD) known to date [1]. The underlying pathogenesis of atherosclerosis is manifested by oxidative stress, chronic inflammation, dyslipidemia, hyperglycemia, and shear stress (physical effect) [2]. Due to the high compositions of cholesterol, cholesteryl esters (CE) (approximately 50% of the total composition), and phospholipids in low density lipoprotein (LDL), it is prone to oxidation mediated by reactive oxygen species (ROS) [3]. Oxidized LDL (OxLDL) acts as a pro-inflammatory and pro-atherogenic modulator that initiates endothelial dysfunction and triggers inflammatory responses via monocyte-derived macrophage-mediated synthesis and secretion of inflammatory cytokines. These abnormalities promote recruitment and subsequent activation of macrophages, and intracellular lipid accumulation within atherosclerotic lesions [4, 5].

* Corresponding author.
E-mail address: eijimatu@md.okayama-u.ac.jp (E. Matsuura).

https://doi.org/10.1016/j.heliyon.2020.e05743
Received 23 September 2020; Received in revised form 28 October 2020; Accepted 11 December 2020

Hippocrates's '*let food be thy medicine and medicine be thy food*' ideology has been receiving growing interest in recent years [6]. Many individuals have turn to functional food as a source of natural remedy to complement the physiological system in health promotion and disease management. These exogenous antioxidants support the physiological endogenous antioxidant mechanism against oxidative injuries and foster restoration of redox homeostasis [7]. Thus, the use of exogenous natural antioxidants as a strategy to mitigate inadvertent physiological oxidative damage and related inflammatory signaling pathways remains rationale and may offer relevant insights for both prevention and management of chronic diseases.

Rice has been long known as one of the vital agricultural commodities in staple food markets, providing sources of energy and nourishments to most Asian populations [8]. Rice bran, the agricultural byproduct of rice milling, is known to house polyphenols, vitamins, minerals, and proteins [9]. In spite of its nutraceutical potentials, rice bran remains largely under-utilized, still primarily used for animal feeding with only a small portion being used to produce rice bran oil for human consumption [10]. Presently, interest in health attributes of rice bran as functional food has been intensified with focuses primarily centered on the evaluation of rice bran antioxidants in management of health and wellness. Some of the recently reported health attributes of rice bran were associated with its potent anti-atherogenic [11, 12, 13, 14, 15], chemopreventive [16, 17], hypoglycemic [18], anti-hypertensive, and hypocholesterolemic [19, 20] properties.

Since then, the innovative utilizations of rice bran in food industries to tackle adversities arising from issues relating to malnutrition and chronic diseases began to gain public acceptance [21]. Given that oxidative stress and pro-inflammatory-related mechanisms prominently exacerbate the progression of atherosclerosis through interplays of innate and adaptive immune systems, dietary intervention of natural plant-based functional food capable of addressing these impediments remains a point-of-interest. As such, present study was aimed to evaluate the bioactivities and ameliorative effects of rice bran extracts (RBE) derived from selected Japanese rice varieties in modulating the underlying pathogenesis of atherosclerosis via *in vitro* and *in vivo* assay models.

2. Methodology

2.1. Preparation of RBE

A total of 9 different colored rice varieties of *Oryza sativa* L. species and japonica cultivar group were locally sourced in Japan. Phytochemical profiles and bioactivities of RBE derived from these colored rice varieties were pre-screened and RBE derived from two selected rice varieties were used for this study. The two selected colored rice varieties were: (1) red rice ('Tanegashima-uruchi' – Romanized name in Japanese, from Tanegashima, Kagoshima, Japan) and (2) purple-black rice ('Shikokumai' or 'Kuromai' – Romanized name in Japanese, from Yakage, Okayama, Japan) (Figure 1). Prior to rice milling, rice grains were pre-stabilized by heat-drying at 100 °C for 30 min to deactivate lipase. The resulting bran powder from the milling process was sieved through a 0.35 mm sieve and stored at -80 °C until use. RBEs were prepared via simple solvent extraction method [22]. Briefly, rice bran powder was soaked in absolute methanol (MetOH) at a weight-to-volume ratio (w/v) of 1:20. The extractions were carried out in a culture shaker at a constant temperature of 25 °C with gentle shaking (120 ms^{-1}) for 24 h. The extracts were then filtered through chromatography filter paper (Advantec Chromatography Filter Paper Grade 51B, Cole-Parmer, Vernon Hills, IL, USA), and concentrated under reduced pressure via rotary evaporator. All extracts were dried under constant stream of nitrogen (N_2) gas and stored at -22 °C until use. Dried extracts were reconstituted in absolute ethanol (EtOH) to desirable concentration, in units of weight of dried extract/volume of EtOH (w/v) for subsequent phytochemical profiling and bioactivity assays. RBE derived from red and purple rice varieties in subsequent context of the manuscript were annotated as 'R.RBE' and 'P.RBE' respectively.

2.2. Phytochemical profiling of RBE

Phenolics, flavonoids, anthocyanins, pro-anthocyanidins, gamma oryzanol (γ-oryzanol) and vitamin E (tocopherols and tocotrienols) contents of RBEs were determined via colorimetric and chromatographic assays.

2.2.1. Phenolics contents

Phenolics contents of RBEs were determined as per method of Singleton and Rossi (1965) [23] with minor modifications. Briefly, diluted rice bran extracts were mixed with 7.5 % (w/v) sodium carbonate (Na_2CO_3) and Folin-Ciocalteu reagent (diluted 10 folds) in a 96-well microplate. The reaction mixtures were left to incubate at room temperature for 60 min before absorbance was measured at 650 nm via a microplate reader (Sunrise™, Tecan Trading AG, Männedorf, Switzerland). Gallic acid was used as reference standard and the phenolic contents of RBEs were expressed in mg of gallic acid equivalents (GAE) per 100 g of dried extract.

2.2.2. Flavonoids contents

Flavonoids contents of RBEs were assessed via aluminium complexation reaction as per methods of Jia et al. (1999) [24] and Herald et al. (2012) [25] with minor modifications. Briefly, RBEs were pre-mixed with ultra-pure water and 5 % (w/v) of sodium nitrite ($NaNO_2$). The reaction mixtures were homogenized thoroughly for 5 min before 10 % (w/v) aluminium trichloride ($AlCl_3$) was added and incubated for 10 min at room temperature. Then, a mixture of 1 M sodium hydroxide (NaOH) and ultra-pure water (1:1 ratio) was added to the reaction mixtures. Samples were centrifuge at 3,000 rpm for 5 min at room temperature to remove precipitates. Lastly, the absorbances of collected supernatants were measured at 510 nm via UV-Visible spectrophotometer (Cary 50 Conc UV-Visible Spectrophotometer, Varian, Inc., Palo Alto, CA, USA). Quercetin was used as reference standard and the flavonoid contents of

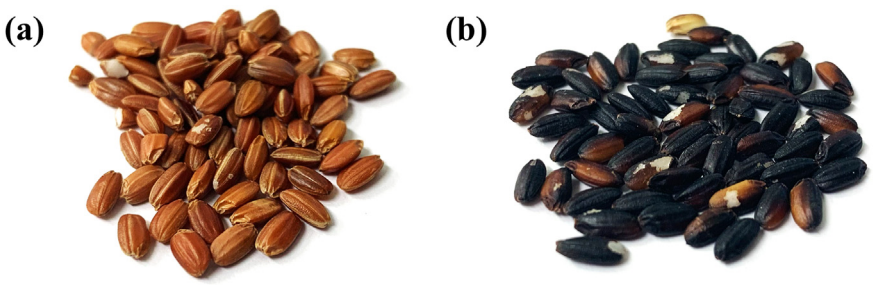

Figure 1. Rice grains of (a) 'Tanegashima-uruchi' – Romanized name in Japanese (red rice) and (b) 'Shikokumai' or 'Kuromai' – Romanized name in Japanese (purple-black rice).

RBEs were expressed in mg of quercetin equivalents (QE) per g of dried extract.

2.2.3. Anthocyanins contents

Anthocyanins contents of RBEs were determined through pH differential method as per method of Giusti and Wrolstad (2001) [26] with minor modifications. Briefly, RBEs were pre-mixed with 0.024 M potassium chloride (KCl) (pH 1.0) in a 96-well microplate and incubated at room temperature for 15 min. Absorbances were then measured at 490 nm and reference wavelength at 650 nm respectively. Content of additional 96-well microplate was set up by mixing RBEs and 0.4 M sodium acetate (NaOAc) (pH4.5) and also incubated at room temperature for 15 min. Absorbances were then measured at 490 nm and reference wavelength at 650 nm respectively. Anthocyanin contents of RBEs were determined through the following Eqs. (1) and (2):

$$\text{Absorbance} = (A_{490nm} - A_{650nm})_{pH1.0} - (A_{490nm} - A_{650nm})_{pH4.5} \quad (1)$$

Eq. (1) determines the variations in absorbances between two pH buffer systems

$$\text{Anthocyanins contents} = \frac{A\ x\ MW\ x\ DF\ x\ 1000}{MA\ x\ 1} \quad (2)$$

Eq. (2) determines anthocyanin content of sample in unit of mg cyanidin-3-glucoside equivalent per mass of sample, in which:

A = Difference in Absorbance from equation (1)
MW = Molecular weight of cyanidin-3-glucoside (C3G) (449.2 g/mol*)*
DF = Sample dilution factor
MA = Molar absorptivity (equivalent to 26900 L/mol·cm)

2.2.4. Pro-anthocyanidins contents

Pro-anthocyanidins contents of RBEs were determined through high-throughput vanillin assay as per method of Herald et al. (2014) [27] with minor modifications. Briefly, reference standard catechin (0.02–2.50 mg/mL; in EtOH), RBEs (1 mg/mL), and negative control (EtOH only) were respectively loaded to 96-well microplate and subsequently mixed with working vanillin solution [consisting of 1 part of 1 % (w/v) vanillin solution in EtOH and 1 part of 25 % (v/v) H_2SO_4 in EtOH]. In order to eliminate false positives, background checks were conducted by checking absorbances of reaction mixtures containing standard/samples/negative control and background check solution (consisting of 1 part of EtOH and 1 part of 25 % (v/v) H_2SO_4 in EtOH). All reaction mixtures were left to incubate at 30 °C for 20 min and absorbance was measured at 490 nm. Pro-anthocyanidin contents of RBEs were expressed in mg catechin equivalent per kg of dried extract and were determined via the following Eq. (3).

$$\text{Pro-anthocyanidins contents} = (A_{sample} - A_{reagent\ blank}) - (A_{background} - A_{background\ reagent\ blank}) \quad (3)$$

Where:

A_{sample} *= Reference standard (catechin)/RBEs + [1 % (w/v) vanillin-EtOH + 25 % (v/v)* H_2SO_4 *in EtOH]*
$A_{reagent\ blank}$ *= EtOH + [1 % (w/v) vanillin-EtOH + 25 % (v/v)* H_2SO_4 *in EtOH]*
$A_{background}$ *= Reference standard (catechin)/RBEs + [EtOH + 25 % (v/v)* H_2SO_4 *in EtOH]*
$A_{background\ reagent\ blank}$ *= EtOH + [EtOH +25 % (v/v)* H_2SO_4 *in EtOH]*

2.2.5. Gamma oryzanol (γ-oryzanol) contents

Total γ-oryzanol contents of RBE were determined spectrophotometrically as per method of Bucci et al. (2003) [28] with slight modification. Briefly, the analysis was performed by using a UV-Visible spectrophotometer (UV-2700, Shimadzu Corp., Kyoto, Japan). Maximum absorption spectrum of γ-oryzanol was determined at 328 nm. Different concentrations of γ-oryzanol standards were used to establish a reference calibration curve and the total γ-oryzanol content of RBE were expressed in unit of mg of γ-oryzanol per g of dried extract.

2.2.6. Vitamin E

Vitamin E contents of RBE were determined via a reversed phase high performance liquid chromatography (HPLC) system (Agilent 1260 Infinity LC, Agilent Technologies, Santa Clara, CA, USA) coupled with a fluorescence detector (Agilent 1260 Infinity Fluorescence Detector, Agilent Technologies, Santa Clara, CA, USA). Briefly, diluted stock concentrations of RBEs (5 mg/mL) were prepared in HPLC grade methanol. All samples were filtered through 0.45 μm PTFE filter prior to sample injection into HPLC. A solvent system consisting of 100 % HPLC grade methanol was delivered to a 4.6 × 250 mm, 5 μm C-18 column (Zorbax SB-C18, Agilent Technologies, Santa Clara, CA, USA). Separation of vitamin E isomers was performed in isocratic elution mode at a flow rate of 1.0 mL/min and column temperature were kept at 25 °C. A sample injection volume of 10 μL was injected into the HPLC and the vitamin E derivatives were detected at the excitation and emission wavelengths of 296 nm and 330 nm respectively. Tocomin50, a mixture of tocotrienols and tocopherol derived from palm oil was used as reference standard.

2.3. In vitro antioxidant capacity assessments

Chemical free radicals: 2,2-diphenyl-1-picrylhydrazyl (DPPH), 2,2′-azino-di-3-ethylbenzthiazoline sulfonic acid (ABTS), and hydrogen peroxide (H_2O_2) were used to evaluate the antioxidant capacities of RBEs.

2.3.1. 2,2-Diphenyl-1-picrylhydrazyl (DPPH) free radical scavenging assay

DPPH free radical scavenging assay was performed as per method of Herald et al. (2012) [24] with minor modifications. Briefly, serially diluted RBEs (15.6 μg/mL–1000 μg/mL) were mixed with 0.4 mM DPPH working solution in a 96-well microplate. The reaction mixture was left for incubation at room temperature for 30 min (away from light) and absorbance was then measured at 490 nm via a microplate reader (Sunrise™, Tecan Trading AG, Männedorf, Switzerland). Vitamin C, quercetin, and gallic acid were used as positive controls. EtOH was used as negative control and reagent blank. DPPH free radical scavenging capacities of RBEs were determined by identifying the inhibitory concentrations (IC_{50}) of RBEs required to reduce the absorbance of DPPH free radical solution by 50 %.

2.3.2. 2,2′-azino-di-3-ethylbenzthiazoline sulfonic acid (ABTS) scavenging capacity assay

ABTS scavenging capacities of RBEs were evaluated as per method of Miller et al. (1993) [29] with slight modifications. ABTS radical solution was pre-prepared by mixing 2.45 mM potassium persulfate solution and 7 mM ABTS solution at equal ratio, incubated in the dark at room temperature for 12 h. The resulting reaction solution was further diluted 10x with EtOH (until an initial absorbance of approximately 0.700 A.U. at 734 nm was attained before use). Working solution of ABTS was then added to serially diluted RBEs (15.6 μg/mL–1000 μg/mL), and positive controls: vitamin C, quercetin, and gallic acid respectively. EtOH was use as negative control and reagent blank. Reaction mixtures were left to incubate at room temperature, in the dark for 10 min. Absorbance was measured at 734 nm via a microplate reader (FlexStation 3, Molecular Devices, LLC., San Jose, CA, USA). ABTS free radical scavenging capacities of RBEs were determined by identifying the IC_{50} concentrations of RBEs required to reduce the absorbance of ABTS radical solution by 50%.

2.3.3. Hydrogen peroxide (H_2O_2) scavenging assay

H_2O_2 scavenging capacities of RBEs were determined via a modified enzymatic colorimetric assay as per method of Fernando and Soysa (2015) [30] with minor modifications. Briefly, reaction mixtures consisting of phenol-aminoantipyrine solution (0.17 M phenol and 2.46 mM

4-aminoantipyrine), 1 mM H_2O_2, and serially diluted test samples in pH 7.0 phosphate (PBS) buffer were prepared and loaded onto a 96-well microplate. Vitamin C, quercetin, and gallic acid were used as positive controls. PBS buffer was used as negative control and reagent blank. The resulting reaction mixtures were left at room temperature to incubate for 5 min and subsequently followed by the addition of 37.5 U/mL (final concentration in reaction mixture: 1.5 U/mL) horseradish peroxidase (HRP). Reactions were then carried out at 37 °C for 30 min and absorbance was measured at 490 nm via a microplate reader (Sunrise™, Tecan Trading AG). H_2O_2 scavenging capacities of RBEs were determined by identifying the IC_{50} of RBEs required to reduce the initial absorbance of reaction mixture by 50%.

2.4. Cell culture

Murine J774A.1 macrophage-like cell (Riken BioResource Research Center, Ibaraki, Japan) was used as mammalian cell culture model for *in vitro* mammalian cell culture-based assays. Cells were maintained in DMEM supplemented with 10 % (v/v) fetal bovine serum (FBS) and 100 units/mL of penicillin-streptomycin.

2.4.1. Cell cytotoxicity

J774A.1 macrophage-like cells were seeded onto a 96-well microplate at a density of 5×10^3 cells per well and pre-incubated for 24 h prior to RBE treatment. Cells were then treated with different concentrations of serially diluted RBEs (15.625 μg/mL – 250 μg/mL) for 24, 48, and 72 h respectively. EtOH composition in DMEM of prepared RBEs for cell treatment was kept below 1% (v/v) while 1% (v/v) EtOH in DMEM, a concentration of EtOH that did not incur cytotoxicity to J774A.1 macrophage-like cells was used as negative control. Cell cytotoxicity of RBEs on J774A.1 macrophage-like cells were examined through Cell Counting Kit-8 (CCK-8) (Dojindo Molecular Technologies Inc., Kumamoto, Japan) as per kit's instructions. The absorbance was measured through a microplate reader (Sunrise™, Tecan Trading AG) at 490 nm and a reference wavelength of 600 nm.

2.4.2. Anti-inflammation assay (Griess assay)

J774A.1 macrophage-like cells were seeded at a density of 1×10^5 cells per well onto a 24-well plate and pre-incubated for 24 h prior to cell treatment. LPS from *Escherichia coli* 0127:B8 (Sigma-Aldrich, Inc., Darmstadt, Germany), at a final concentration of 1 μg/mL, was used as an inflammatory inducer. Cells were first treated with different concentrations of RBEs (62.5 μg/mL – 250 μg/mL) for 4 h, then co-incubated with LPS for another 20 h. After 24 h of co-incubations with RBEs and LPS, cell culture supernatants were collected by centrifugation at 1,500 rpm, room temperature for 5 min. Anti-inflammatory capacities of RBEs were evaluated via the Griess assay, a colorimetric assay that measures nitrite, a stable metabolite from oxidation of nitric oxide (NO) radicals [31]. Briefly, cell culture supernatants were mixed with Griess reagent, consisting of 1 part of 1 % (w/v) sulfanilamide in 5 % (v/v) phosphoric acid (H_3PO_4) and 1 part of 0.1 % (w/v) N-1-napthylethylenediamine dihydrochloride (NED). Sodium nitrite (0.78 μM–50 μM) was used as reference standard. Reactions were carried out at room temperature for 20 min and absorbance was measured at 570 nm via a microplate reader (Sunrise™, Tecan Trading AG). The % NO production relative to non-RBE treated LPS control was determined through the following Eq. (4):

$$\% \text{ NO Production} = (NO_2^-{}_{\text{ sample}} / NO_2^-{}_{\text{ control}}) \text{ x } 100 \quad (4)$$

Where:

NO_2^- refers to concentration of nitrite (NO_2^-) determined through sodium nitrite reference standard curve

$NO_2^-{}_{sample}$ = Concentration of nitrite (NO_2^-) in groups treated with RBE/non-RBE, non-LPS negative control group

$NO_2^-{}_{control}$ = Concentration of nitrite (NO_2^-) in non-RBE treated LPS control group

2.4.3. Gene and protein expressions of inflammatory cytokines/modulators

J774A.1 macrophage-like cells were seeded at a density of 5×10^5 cells per well onto a 6-well plate and pre-incubated for 24 h prior to cell treatment. Cells were first treated with two different concentrations of RBEs (62.5 μg/mL & 125 μg/mL) for 4 h, then followed by LPS (1 μg/mL) stimulation for 20 h. After 24 h of co-incubations with RBEs and LPS, cells were then processed accordingly for gene and protein expressions-related studies.

Total RNA from cells was extracted using PureLink™ RNA mini kit (ThermoFisher Scientific, Carlsbad, CA, USA) as per kit's instructions. Concentration and purity of isolated total RNA were assessed by using BioSpec-nano (Shimadzu Corp., Kyoto, Japan). Reverse transcription of total RNA to single stranded cDNA was performed using High-Capacity RNA-to-cDNA™ kit (ThermoFisher Scientific). Quantitative PCR (qPCR) was performed on Applied Biosystems StepOnePlus Real-Time PCR system (ThermoFisher Scientific) based on SYBR green chemistry (ROX as passive reference dye) from Applied Biosystems PowerUP™ SYBR™ green master mix (ThermoFisher Scientific). Expression profiles of targeted genes: inducible nitric oxide synthase (iNOS), tumour necrosis factor α (TNF-α), interleukin 1 alpha (IL-1α), interleukin 1 beta (IL-1β), and interleukin-6 (IL-6) were measured through comparative C_T using their respective primer sequences (Table 1). Expression levels of targeted genes were normalized against reference control gene glyceraldehyde 3-phosphate dehydrogenase (GAPDH). The qPCR running condition began with holding steps at 50 °C for 2 min and followed by 95 °C for 2 min, then PCR cycles continued sequentially for 40 cycles at 95 °C for 15 s, 58 °C for 30 s, and 72 °C for 60 s.

For protein extraction, cells were dislodged by cell scrapper and centrifuged (2000 rpm, 4 °C, 5 min) to collect cell pellet. After washing with ice-cold PBS buffer, cell pellets were suspended in ice-cold lysis buffer [20 mM Tris-HCl, pH7.5, 150 mM NaCl, 5 mM EDTA, 5 mM EGTA, 1 % (v/v) NP-40, 0.1 % (w/v) SDS, 0.1% (w/v) sodium deoxycholate, 20 mM β-glycerophosphate, 2 mg/mL NaF, and 0.18 mg/mL Na_3VO_4] supplemented with protease inhibitor cocktail P8340 (Sigma-Aldrich, Inc.). Reaction was then incubated at 4 °C for 30 min. Supernatant of homogenate was collected via centrifugation (15,000 rpm, 4 °C, 15 min) and protein content of extract was determined through Pierce™ BCA Protein Assay Kit (ThermoFisher Scientific). Collected proteins were denatured with SDS-polyacrylamide gel electrophoresis (SDS-PAGE) sample buffer (supplemented with 2-mercaptoethanol as reducing agent) at 99 °C, for 5 min prior to SDS-PAGE. After SDS-PAGE, proteins on gel were then wet transferred onto 0.2 μm ClearTrans® nitrocellulose membranes (Fujifilm Wako Pure Chemical Corp., Osaka, Japan). Membranes were blocked with 5 % (w/v) skim milk suspended in TBS-T buffer [10 mM Tris-HCl (pH 7.4), 150 mM NaCl, and 0.05% Tween20] at room temperature, for 1 h. After three washings with TBS-T buffer, membranes were incubated at 4 °C, overnight with primary antibodies: iNOS (D6B6S) (#13120S, Cell Signaling Technology, Inc., Danvers, MA, USA), TNF-α ((#3707S, Cell Signaling Technology, Inc.), IL-1α (D4F3S) (#50794S, Cell Signaling Technology, Inc.), IL-6 (D5W4V) XP® (#12912S, Cell Signaling Technology, Inc.), and housekeeping loading control β-actin (13E5) (#4970S, Cell Signaling Technology, Inc.). Primary antibodies were all diluted (1:1000) in 5 % (w/v) bovine serum

Table 1. Primer sequences of targeted genes.

Gene Targets	Forward Primer Sequence (5′-3′)	Reverse Primer Sequence (5′-3′)
iNOS	CAGATCCCGAAACGCTTCA	TGTTGAGGTCTAAAGGCTCCG
TNF-α	CACGCTCTTCTGTCTACTGA	CACTTGGTGGTTTGCTACGA
IL-1α	CGCTTGAGTCGGCAAAGAAA	GAGAGAGATGGTCAATGGCAGA
IL-1β	GCCACCTTTTGACAGTGATGA	ATGTGCTGCTGCGAGATTTG
IL-6	ATGGATGCTACCAAACTGGAT	TGAAGGACTCTGGCTTTGTCT
GAPDH	AACTTTGGCATTGTGGAAGG	ACACATTGGGGGTAGGAACA

albumin suspended in TBS-T buffer. After three washings with TBS-T buffer, membranes were then incubated with diluted HRP-linked secondary antibody (1:2000) (#7074S, Cell Signaling Technology, Inc.) in 5 % (w/v) skim milk-TBS-T buffer, at room temperature for 1 h. Immunoreactive protein bands on membrane were treated with ImmunoStar® LD substrate (Fujifilm Wako Pure Chemical Corp.) and visualized on Amersham Hyperfilm™ ECL (GE Healthcare Ltd., Buckinghamshire, UK). Optical density plots and relative densities of protein bands were determined through ImageJ software analysis.

2.5. *In vivo* study

All animal-related experimental protocols were approved by Animal Care and Use Committee of Okayama University (OKU-2019389). Low density lipoprotein receptor knockout mice (B6.129S7-*Ldlr*^{tm1Her}/J) (*Ldlr*$^{-/-}$ mice) were purchased from Jackson Laboratory (Bar Harbor, ME, USA). Five mice were housed per cage in a temperature- and light- (daily photoperiod of 12 h) controlled animal facility. Mice were fed with normal chow diet (ND) (MF, Oriental Yeast, Co. Ltd., Tokyo, Japan) until 8 weeks of age. Westernized high fat diet (HFD) containing 2% cholesterol and 0.5% cholic acid (Oriental Yeast, Co. Ltd.) was used for diet-induced atherosclerosis in mice (Table 2). At 8 weeks of age, 32 male mice were randomly and equally assigned to 4 groups (n = 8 per group), and fed with: (a) ND; (b) HFD; (c) HFD + R.RBE (10 % w/w); (d) HFD + P.RBE (10 % w/w) diets respectively for 12 weeks. Powdered HFD were pre-mixed with respective lyophilized RBE, at 10 % (w/w) composition. Mice were given ad libitum access to food and water. Fresh animal feed was replaced weekly. Initial body weights of mice were measured and were subsequently recorded weekly throughout the experimental duration. Fasting whole blood samples (6 h fasting) of mice were collected through lateral tail veins every 3 weeks with sodium citrate buffer (Sysmex Corp., Kobe, Japan) as anti-coagulant. Blood plasmas were collected through centrifugation of whole blood samples at 1,000 *g*, 4 °C for 15 min. At 20 weeks of age, terminal blood collection from posterior vena cava was performed. Biological specimens such as aortas, livers, and aortic sinuses were collected for downstream bioassays.

2.5.1. *Plasma lipid profiling*

Commercial enzymatic assay kits: LabAssay™ cholesterol (Fujifilm Wako Pure Chemical Corp.) and LabAssay™ triglyceride (Fujifilm Wako Pure Chemical Corp.) were used to assess the levels of plasma cholesterol and triglycerides. Assays were performed as per kits' instructions. Absorbance was measured via a microplate reader (Sunrise™, Tecan Trading AG).

2.5.2. *En face preparation and analysis of mouse aortas*

A separate group of 24 male *Ldlr*$^{-/-}$ mice was used for en face analysis of aortas. At 8 weeks of age, mice were randomly and equally assigned to 4 groups (n = 6 per group). Each group of mice was treated similarly and fed with respective types of diet stipulated in section '2.5 *In vivo* study' of 'Methodology' for 12 weeks. Mouse aortas were excised at endpoint. After terminal blood collection from posterior vena cava, mouse aorta was first perfused with PBS, then followed by 10 % neutral buffered formalin. The aorta was cleaned through careful removal of surrounding adventitial fat tissues and was then fixed in 10 % neutral buffered formalin at 4 °C overnight. Fixed aortas were stained with Oil Red O (ORO) stain for neutral lipids and were then dissected longitudinally [32] for en face analysis. Images of en face aortas were captured via Olympus SZX12 stereoscopic microscope (Olympus Corp., Tokyo, Japan) equipped with Olympus DP72 (Olympus Corp.) charged-coupled device (CCD) camera. Quantifications of stained lesions in aortas were estimated through ImageJ software analysis.

2.5.3. *Preparation of LDL, oxLDL and oxLDL/β2GPI complexes*

LDL was isolated from a separate group of *Ldlr*$^{-/-}$ mice for preparation of oxLDL and oxLDL/β2GPI complexes. LDL fraction was isolated through a three-step sequential ultracentrifugation process. Briefly, mouse plasma sample was pre-mixed with 200 mM EDTA (to a final concentration of 0.25 mM EDTA). Three parts (~750 μL) of plasma/EDTA mixture was

Table 2. Compositions of westernized high fat diet (HFD).

Components	Composition (%)
Casein	19.82
L-cystine	0.3
Maize Starch	3.7458
Pregelatinized Maize Starch	1.25
Sucrose	31.65
Soybean Oil	1.0
Powdered Cellulose	5.0
AIN-93 Vitamin Mix	1.0
AIN-93G Mineral Mix	3.5
Choline Bitartrate	0.25
Tertiary Butylhydroquinone	0.0042
Butter Fat	20
Maltodextrin	9.98
Cholesterol	2.0
Cholic Acid	0.5%

loaded to a 1.5 mL polycarbonate (PC) tube and later followed by the addition of 1 part (~250 μL) of 0.25 mM EDTA/PBS, through the side-wall of PC tube to retain phase separation. Centrifugation was then carried out via TL-100 ultracentrifuge (Beckman Coulter, Inc., Fullerton, CA, USA) at 100,000 rpm, 10 °C for 7 min. The VLDL and chylomicron-containing top white layer (~250 μL) was removed through aspiration and 1 part (~250 μL) of fresh 0.25 mM EDTA/PBS was then slowly added into the PC tube. Centrifugation was then again carried out at 100,000 rpm, 10 °C for 2.5 h. Approximately ~250 μL of top white layer was then removed and followed by addition of 150 μL of 0.5 g/mL KBr in 0.25 mM EDTA/PBS buffer. Mixture was homogenized through gentle pipetting. Centrifugation was then again carried out at 100,000 rpm, 10 °C for 5 h. After the third centrifugation step, the top white fraction (LDL-containing fraction) was collected, pooled and dialyzed against PBS buffer to remove both EDTA and KBr.

Chemically oxidized LDL was prepared through copper (II) sulphate ($CuSO_4$)-mediated oxidation as described previously [33]. Briefly, 100 μg/mL of apoB equivalent LDL was oxidized with 5 μM $CuSO_4$ at 37 °C for 12 h. EDTA, at a final concentration of 1 mM was used to terminate the oxidation process. Oxidation status of oxLDL was then assessed through thiobarbituric acid-reactive substance (TBARS) assay and agarose gel electrophoresis respectively [33, 34]. OxLDL/β2GPI complex was prepared as reference calibrator for oxLDL/β2GPI enzyme-linked immunosorbent assay (ELISA). OxLDL and human β2GPI were co-incubated at a ratio of (2:1), at 37 °C for 16 h [20], then stored at -80 °C until use.

2.5.4. OxLDL/β2GPI ELISA

ELISA for murine plasma oxLDL/β2GPI complex was prepared in-house as per method of Ames et al. (2010) [35] and Shen et al. (2011) [36] with slight modifications. Murine monoclonal anti-β2GPI IgG (3H3) was pre-prepared from antibody-producing hybridoma cells as described previously [34]. 3H3 antibody (8 μg/mL) in TBS buffer (10 mM Tris-HCl, 150 mM NaCl, pH 7.4) was coated onto a 96-well microplate (Nunc MaxiSorp™, ThermoFisher Scientific) and incubated at 4 °C overnight. Wells were then blocked with 1 % (w/v) BSA at 4 °C overnight. Murine plasma samples (50-fold dilution) and oxLDL/β2GPI complex reference calibrator (0.04 ng/mL – 25 ng/mL apoB equivalent) were diluted in 0.2 % (w/v) skim milk-TBS buffer, and were then loaded to 3H3-coated microplates. Reaction plates were later incubated at 4 °C overnight. Wells were subsequently incubated with HRP-conjugated anti-mouse LDL IgG [1000-fold dilution in 0.75 % (w/v) skim milk-TBS buffer] at room temperature for 3 h. Wells were washed extensively with 0.05 % (v/v) Tween-20 in 0.01 M PBS buffer at each interval. Color was developed with TMB ELISA substrate (Abcam, Cambridge, UK) and reaction was ceased through addition of 0.3 N H_2SO_4 solution. Absorbance was then measured at 450 nm and 600 nm (reference wavelength) via microplate reader (Sunrise™, Tecan Trading AG). Plasma profile of oxLDL/β2GPI was expressed in units/mL to which 1 unit is equivalent to 0.04 ng/mL of apoB-equivalent oxLDL/β2GPI.

2.6. Histological and immunohistochemical analysis of atherosclerotic lesion in aortic sinus

Excised aortic sinuses were embedded in optimal cutting temperature (O.C.T.) compound (Sakura Finetek, Torrance, CA, USA) and kept at -80 °C until use. Frozen sections of aortic sinuses were serially sectioned (10 μm thickness) via cryostat Leica CM1860 (Leica Microsystems, Solms, Germany) and mounted onto MAS-coated glass slides (Matsunami Glass Industries, Osaka, Japan). For histological staining, the neutral lipids in atherosclerotic lesions was stained with ORO. Frozen serial sections were pre-fixed in 10% neutral buffered formalin for 10 min prior to standard ORO staining protocol. Tissue sections were subsequently counterstained with Mayer's hematoxylin solution (Fujifilm Wako Pure Chemical Corp.) to stain nuclei.

The distributions and localizations of smooth muscle cells, macrophages and oxLDL/β2GPI complex were visualized through immunofluorescence staining. Sectioned tissues were first permeabilized in 0.2 % (v/v) tween-20/PBS buffer for 10 min, then followed by blocking step with Protein Block Serum-Free (Dako North America, Inc., Carpinteria, CA) at room temperature for 2 h. Indirect immunofluorescence staining was applied for detections of smooth muscle cells and macrophages. Sectioned tissues were incubated with primary antibodies: (i) for smooth muscle cells – rabbit anti-α-smooth muscle actin (D4K9N) XP® monoclonal IgG at 1000-fold dilution (Cell Signaling Technology, Inc., Danvers, MA, USA) and (ii) for macrophages – rat anti-mouse CD107b (Mac-3) monoclonal IgG at 100-fold dilution (BD Pharmingen™, BD Biosciences, San Jose, CA, USA), at 4 °C overnight respectively. After incubation, sectioned tissues were labeled with: (i) cyanine 5.5 (Cy5.5)-goat anti-rabbit IgG H&L, at 1000-fold dilution (ab6942, Abcam) – for rabbit anti-α-smooth muscle actin (D4K9N) XP® monoclonal IgG-stained tissues and (ii) rhodamine-goat anti-rat IgG-R, at 200-fold dilution (sc-2093, Santa Cruz Biotechnology, Inc., Dallas, TX, USA) – for rat anti-mouse CD107b (Mac-3) monoclonal IgG stained tissues, at room temperature for 2 h respectively. Section tissues were further counterstained with Hoechst 33258 stain (H3569, ThermoFisher Scientific) at room temperature for 5 min. Sectioned tissues were washed extensively with 0.05 % (v/v) Tween-20 in 0.01 M PBS buffer at each interval.

Direct immunofluorescence staining was applied for the detection of oxLDL/β2GPI complexes. Monoclonal anti-β2GPI IgG (3H3) was pre-labeled with Alexa Fluor™ 750 (SAIVI™ Rapid Antibody Labeling Kit, Alexa Fluor™ 750, ThermoFisher Scientific) as per kit's instructions. Sectioned tissues were stained with Alexa Fluor™ 750-labeled 3H3 monoclonal IgG (100 μg/mL) at 4 °C overnight. Sectioned tissues were then counterstained with Hoechst 33258 stain (H3569, ThermoFisher Scientific) at room temperature for 5 min. Sectioned tissues were washed extensively with 0.05 % (v/v) Tween-20 in 0.01 M PBS buffer at each interval.

Images of ORO- and immunofluorescence-stained tissues were obtained with Keyence BZ-X700 All-in-one fluorescence microscope (Keyence Corp., Itasca, IL, USA).

2.7. Gene expressions of aortic and hepatic inflammatory cytokines/modulators

Excised mouse aortas and livers were pre-rinsed in PBS buffer and followed by gentle perfusion with RNA*later* RNA stabilization reagent (Qiagen, Hilden, Germany). Sectioned tissues were then snap-frozen in liquid nitrogen and stored at -80 °C until use. Total RNA from approximately 100 mg of tissues were extracted with PureLink™ RNA mini kit (ThermoFisher Scientific) as per kit's instructions. Subsequent steps for RNA to cDNA conversion and qPCR analysis were performed similarly as stipulated in section '*2.4.3 Gene and protein expressions of inflammatory cytokines/modulators*'.

2.8. Statistical analysis

Data were expressed as mean ± SEM. For statistical comparisons of multiple groups, one-way analysis of variance (ANOVA) and Dunnet analysis (as post-hoc test) were used (GraphPad Prism 8, GraphPad Software, Inc., San Diego, CA, USA). Two tailed and unpaired t-test was used to determine significant differences between two groups. Data were considered statistically significant with $p < 0.05$.

3. Results and discussions

3.1. Phytochemical profiles and antioxidant capacities of RBEs

Both R.RBE and P.RBE showed dissimilar phytochemical profiles (Figure 2). R.RBE possessed higher contents of phenolics and flavonoids as compared to P.RBE (Figures 2a & 2b). As both RBEs were derived from pigmented rice varieties, anthocyanidins (Figure 2c) and pro-

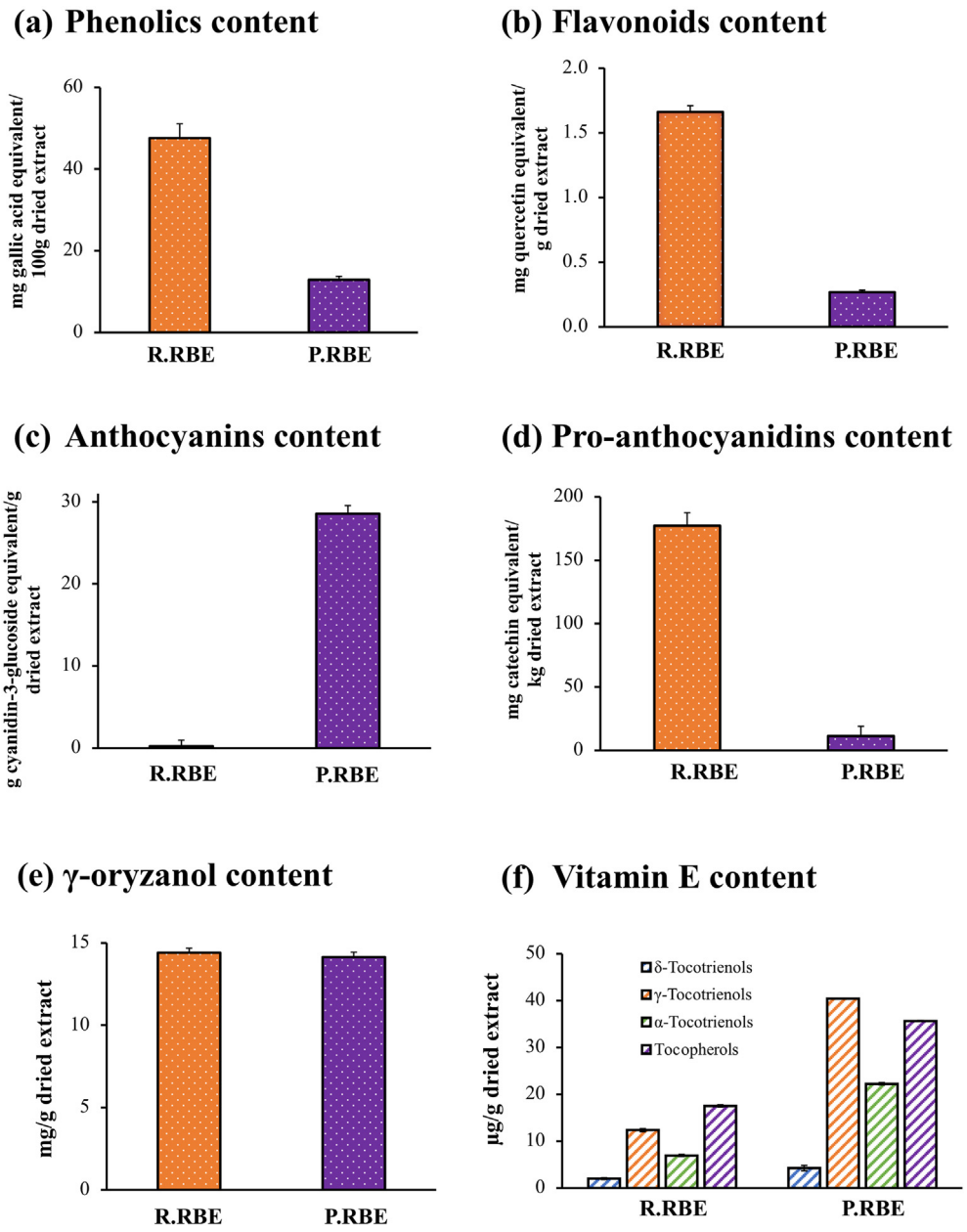

Figure 2. Phytochemical profiles of R.RBE and P.RBE. Contents of selected bioactive compounds: (a) phenolics, (b) flavonoids, (c) anthocyanins, (d) pro-anthocyanidins, (e) γ-oryzanol, and (f) vitamin E in R.RBE and P.RBE were assessed. Data are expressed as mean ± SEM (n = 3).

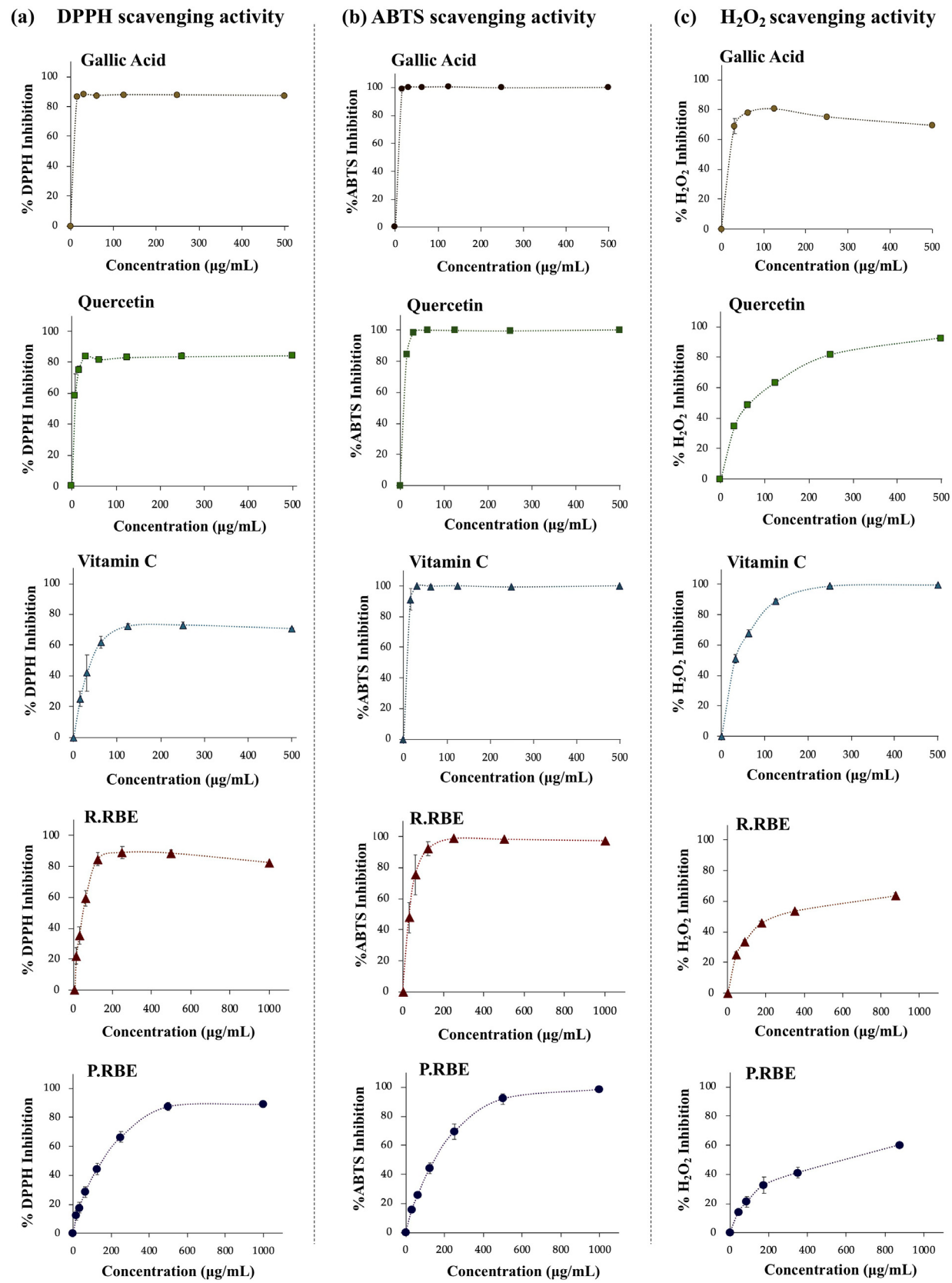

Figure 3. Concentration-response curves of *in vitro* free-radical scavenging capacity assays. Chemical free radicals: (a) DPPH; (b) ABTS; (c) H_2O_2 were used to assess *in vitro* free-radical scavenging capacities of R.RBE and P.RBE. IC_{50} values of RBEs and positive controls (gallic acid, quercetin and vitamin C) were determined through identification of concentrations of test samples required to scavenge free radicals by 50% from respective concentration-response curves. Data are expressed as mean ± SEM (n = 3).

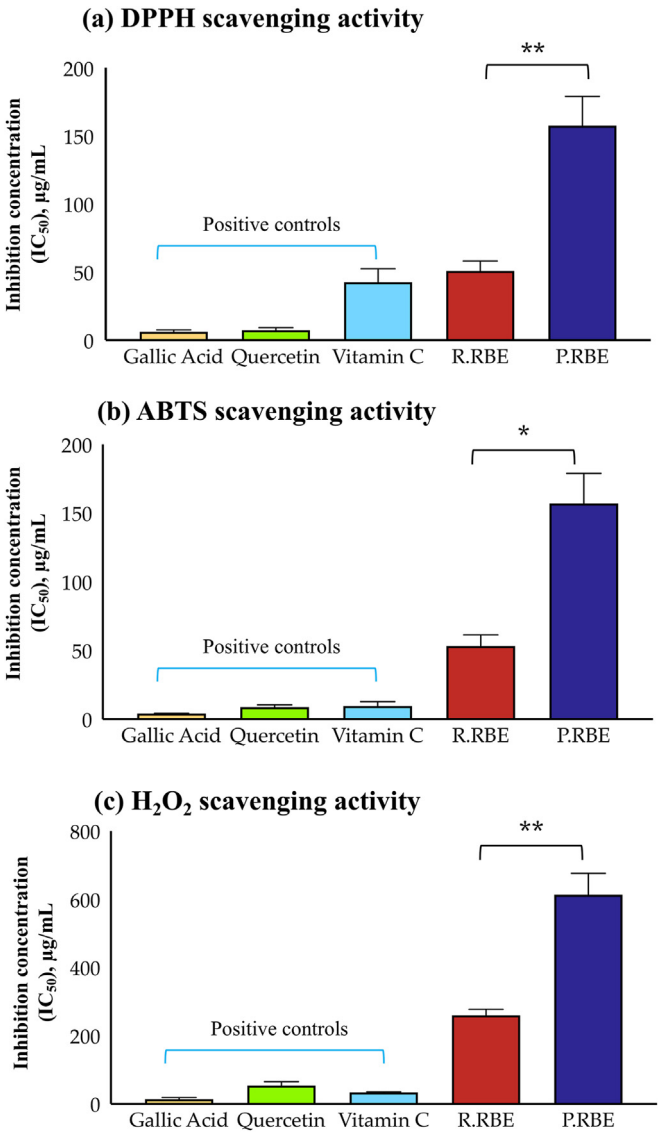

Figure 4. Inhibition concentrations (IC_{50}) of positive controls (gallic acid, quercetin and vitamin C) and RBEs (R.RBE and P.RBE) required to scavenge (a) DPPH, (b) ABTS, and (c) H_2O_2 by 50%. Data are expressed as mean ± SEM (n = 3). Significant differences are represented by: *p < 0.05; **p < 0.01 (two-tailed unpaired t-test).

anthocyanidins (Figure 2d) are distinctive phytochemicals found only in purple-black and red rice respectively. There was no difference in content of γ-oryzanol (Figure 2e) between the two RBEs while P.RBE generally contained higher compositions of targeted vitamin E derivatives as compared to R.RBE (Figure 2f). Although rice brans are generally known to house different natural antioxidants, their respective nutritional diversities and health attributes are affected by their genetic backgrounds and geographic locations [37].

DPPH, ABTS and H_2O_2 were used as sources of chemical radicals to evaluate free-radical scavenging capacities of RBEs. Concentration-response (% inhibition of chemical radicals) curves of free-radical scavenging capacities of RBEs and positive controls were depicted in Figure 3. R.RBE exhibited significantly stronger antioxidant properties as compared to P.RBE in scavenging DPPH ($p < 0.01$), ABTS ($p < 0.05$), and H_2O_2 ($p < 0.05$) chemical radicals (Figures 4a-4c). Overall, R.RBE recorded lower IC_{50} values to scavenge 50% of DPPH (50.76 µg/mL), ABTS (47.48 µg/mL), and H_2O_2 (259.75 µg/mL) as compared to P.RBE at 157.48 µg/mL (DPPH), 135.79 µg/mL (ABTS), and 613.62 µg/mL (H_2O_2) respectively. Polyphenols have demonstrated their antioxidant properties through their free radical scavenging capacities, either by acting as direct hydrogen-donating radical scavengers or attenuate formation of reactive oxygen species (ROS) through suppression of ROS-producing enzymes and upregulation of physiological endogenous antioxidant protective mechanisms [38, 39, 40]. Both R.RBE and P.RBE exhibited free radical scavenging activities through successive inhibitions of DPPH, ABTS and H_2O_2. R.RBE recorded significantly lower IC_{50} values than

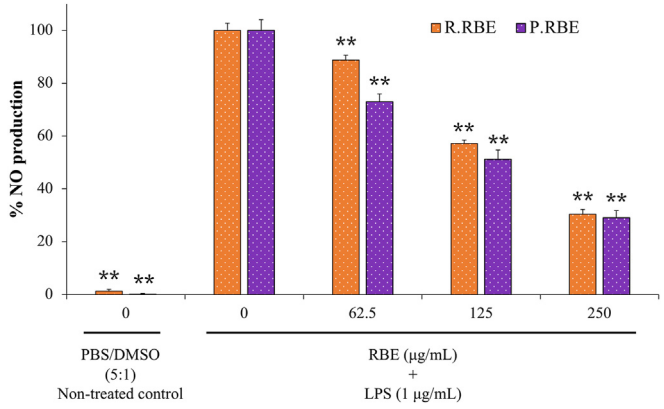

Figure 6. Inhibitory effects of different concentrations of RBEs on NO production in LPS-stimulated J774A.1 macrophage-like cells. Data are presented as means of % NO production relative to non-RBE treated (0 µg/mL) LPS control ±SEM (n = 4). Significant difference is represented by: **p < 0.01 (one-way ANOVA with Dunnett's post-hoc test).

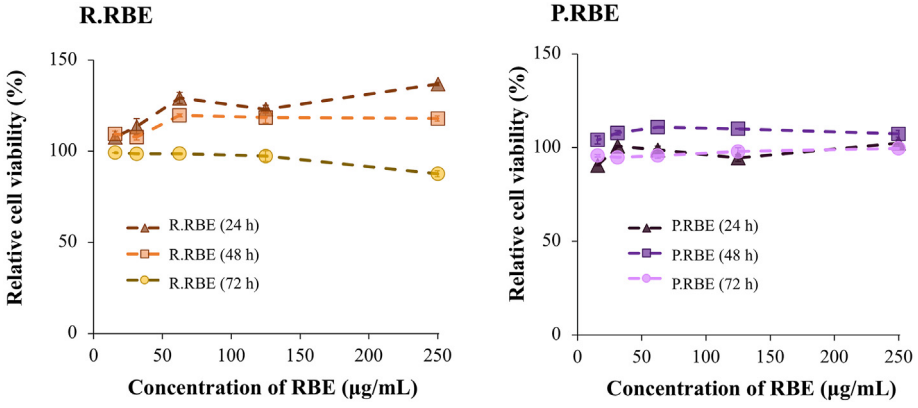

Figure 5. Relative cell viability curves of J774A.1 macrophage-like cells induced with different concentrations of R.RBE and P.RBE over 24, 48 and 72 h respectively. Data are expressed as mean ± SEM (n = 3).

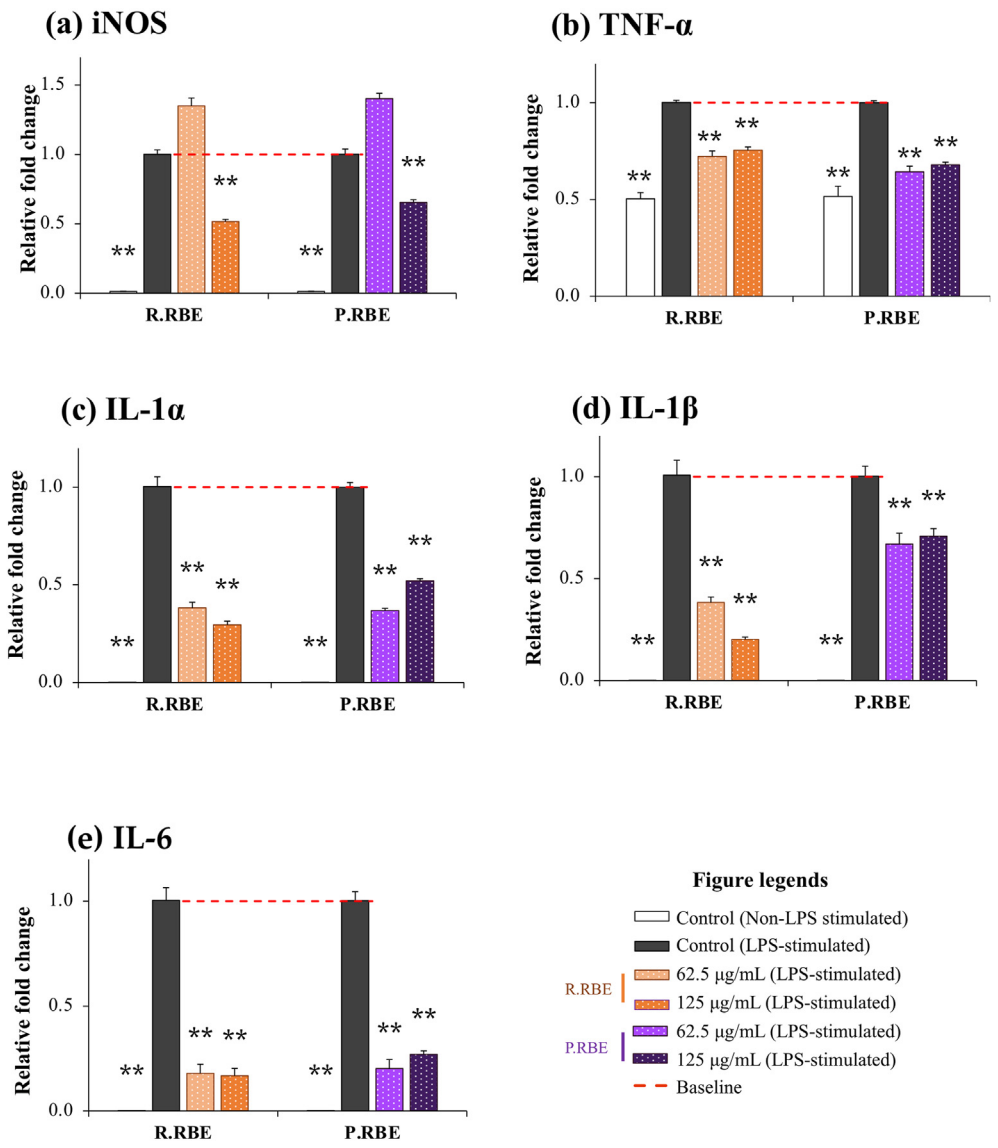

Figure 7. Effects of RBE treatments on gene expressions of (a) iNOS, (b) TNF-α, (c) IL-1α, (d) IL-1β, and (e) IL-6 in LPS-stimulated J774A.1 macrophage-like cells. Expression levels of targeted genes were normalized against reference control gene (GADPH). Data are presented as means of fold changes of mRNA transcripts relative to LPS-stimulated control ±SEM (n = 3). Significant difference is represented by: **p < 0.01 (two-tailed unpaired t-test).

P.RBE to reduce 50% contents of tested chemical radicals. This is likely attributed to the difference in phytochemical profiles of both extracts in which R.RBE possessed higher contents of phenolics and flavonoids than P.RBE.

3.2. Cell cytotoxicity effects of RBE

J774A.1 macrophage-like cells were treated with different concentrations (15.625 μg/mL – 250 μg/mL) of R.RBE and P.RBE over 24, 48, and 72 h. Cell viability was expressed relative to non-RBE treated control. No adverse cytotoxicity effect was observed in RBE-treated J774A.1 macrophage-like cells within the tested concentration range of both RBEs (Figure 5).

3.3. RBEs modulated NO production and expressions of inflammatory cytokines/modulators in LPS-stimulated J774A.1 macrophage-like cells at gene and protein levels

The content of nitrite (NO_2^-), a stable by-product of NO oxidation was measured as an indicator of LPS-stimulated NO production. NO production in LPS-stimulated J774A.1 macrophage-like cells was significantly upregulated as compared to non-treated control (Figure 6). Co-treatments of LPS-stimulated J774A.1 macrophage-like cells with respective R.RBE and P.RBE (for 24 h) significantly suppressed the production of NO in J774A.1 cells. Significant dose-dependent reductions ($p < 0.01$) of NO production by RBEs were recorded in the range between 11% (for lowest concentration of RBE) and 71% (for highest concentration of RBE), with IC_{50} values of R.RBE and P.RBE rated at 155 μg/mL and 129 μg/mL respectively.

LPS stimulated the upregulation in gene and protein expressions of iNOS in stimulated J774A.1 cells (Figure 7a & Figure 8a). Both R.RBE and P.RBE significantly downregulated both gene and protein expressions of iNOS (Figure 7a & Figure 8a) in LPS-stimulated J774A.1 macrophage-like cells. Gene and protein expressions of iNOS in LPS-stimulated J774A.1 cells treated with high concentration of R.RBE and P.RBE (125 μg/mL) were significantly reduced by approximately 35% ($p < 0.01$) and 20% ($p < 0.05$) respectively (as compared to non-RBE treated, LPS-stimulated control).

In addition, the gene expression level of TNF-α, along with other pro-inflammatory cytokines: IL-1α, IL-1β, and IL-6 were also upregulated in

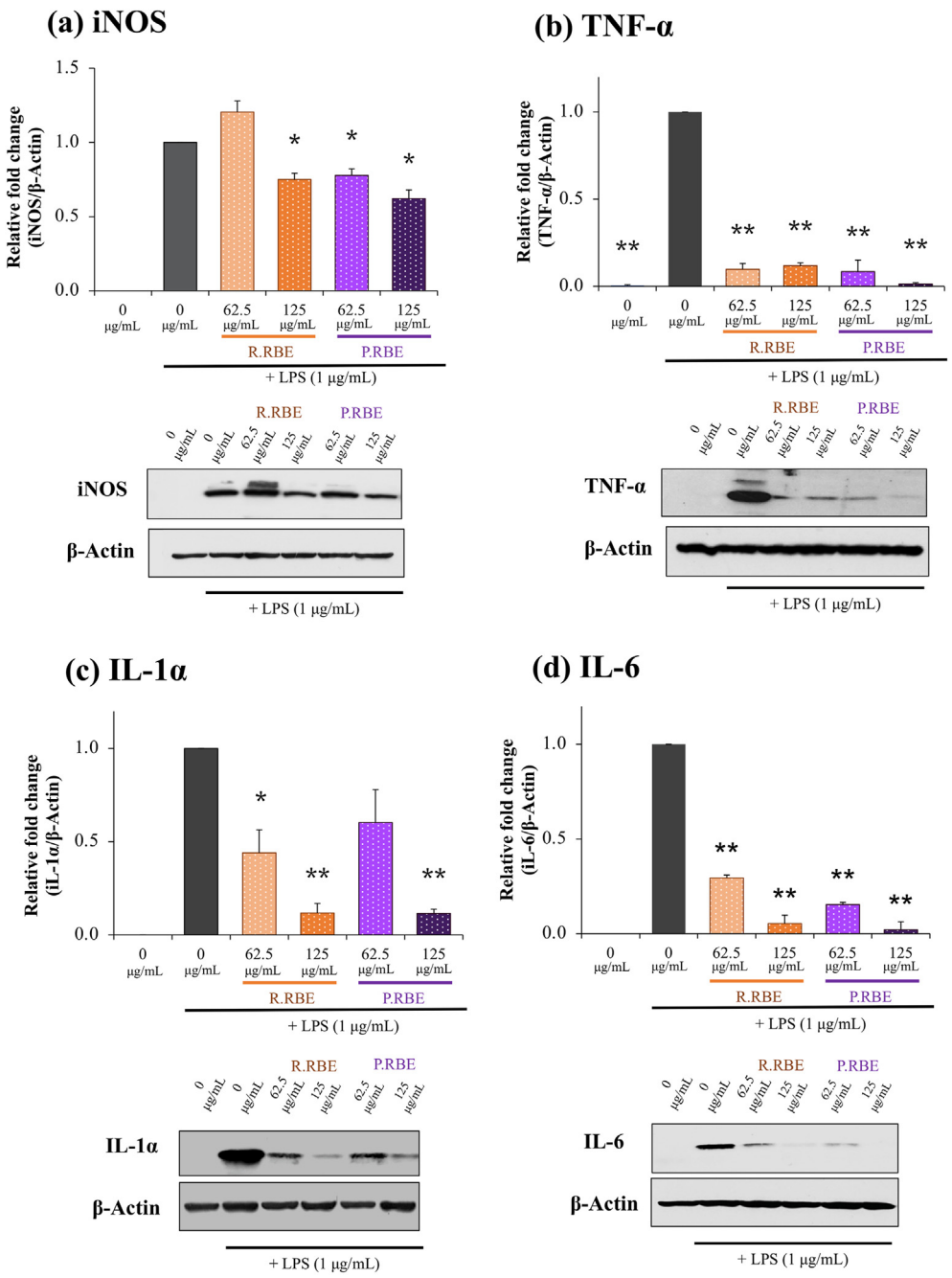

Figure 8. Effects of RBE treatment on protein expressions of (a) iNOS, (b) TNF-α, (c) IL-1α, and (d) IL-6 in LPS-stimulated J774A.1 macrophage-like cells. Expression levels of targeted proteins were normalized against reference control (β-actin). Data are presented as means of fold changes of expressed proteins relative to LPS-stimulated control (0 µg/mL) ± SEM (n = 3). Significant differences are represented by: *p < 0.05; **p < 0.01 (two-tailed unpaired t-test). Corresponding images of developed gel blots were provided as supplementary data in 'Supplementary A'.

LPS-stimulated J774A.1 macrophage-like cells (Figures 7b-7e). Co-treatments of LPS-stimulated J774A.1 macrophage-like cells with respective R.RBE and P.RBE showed potent anti-inflammatory properties through significant downregulations ($p < 0.01$) in gene expression levels of TNF-α (R.RBE: > 25 %; P.RBE: > 32 % downregulation), IL-1α (R.RBE: > 62 %; P.RBE: > 48 % downregulation), IL-1β (R.RBE: > 62 %; P.RBE: > 29% downregulation), and IL-6 (R.RBE: > 82 %; P.RBE: > 73 % downregulation) as compared to non-RBE treated LPS-stimulated control (Figures 7b-7e). Significant downregulations in protein expression levels of TNF-α (R.RBE: > 87 %; P.RBE: > 91 % downregulation), IL-1α (R.RBE: > 56 %; P.RBE: > 89 % downregulation), and IL-6 (R.RBE: > 70 %; P.RBE: > 84 % downregulation) were also seen in RBE-treated LPS-stimulated group as compared to non-RBE treated LPS control group (Figures 8b-8d).

Atherosclerosis is manifested by chronic inflammation. Aside from oxidative stress and dyslipidemia, macrophages play a central systemic role in regulating different developmental stages of atherosclerosis [41]. Endotoxic effects of LPS is capable of stimulating pro-inflammatory type I (M1) macrophages and trigger acute inflammatory response via activation of Toll-like receptors (TLRs)-mediated signaling pathway [42]. Excessive productions of NO and pro-inflammatory cytokines such as TNF-α, IL-1α, IL-1β, and IL-6 are among the consequences of activated M1 macrophages [38].

Under physiological conditions, the synthesis of NO is regulated by both endothelial NOS (eNOS) and neuronal NOS (nNOS) as a function for vascular homeostasis [43]. Contrarily, the activation of inducible form of NOS (iNOS) is mediated by pro-inflammatory cytokines or mitogenic bacterial stimulus such as LPS which promotes overproduction of NO that are reactive with superoxide (O_2^-) to form peroxynitrite [44]. Present study demonstrated that co-treatments of LPS-stimulated J774A.1 macrophage-like cells with R.RBE and P.RBE suppressed the production of NO and expressions of its producing enzyme, iNOS at both gene and

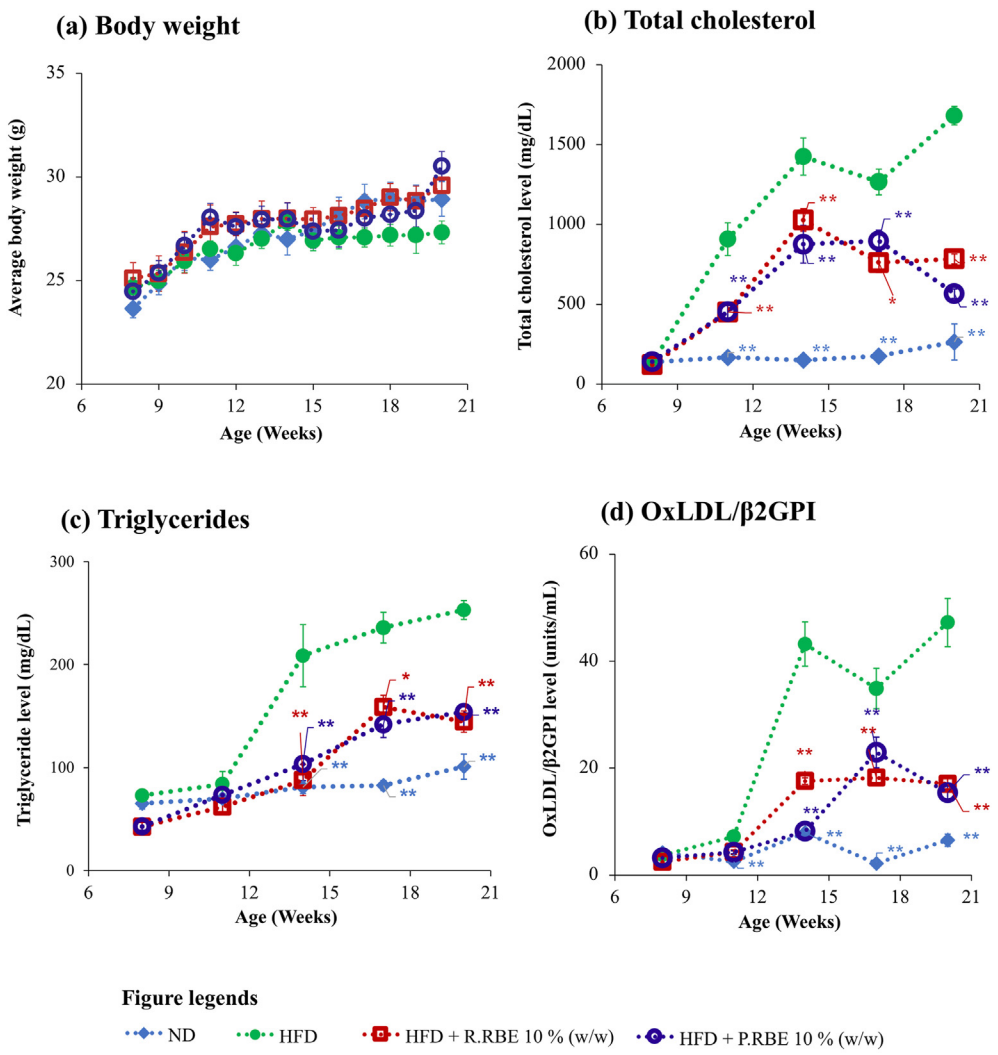

Figure 9. Effects of different diets on (a) body weights, (b) plasma total cholesterol, (c) plasma triglyceride, and (d) plasma oxLDL/β2GPI levels of *Ldlr*$^{-/-}$ mice. *Ldlr*$^{-/-}$ mice were fed with ND, HFD, HFD + R.RBE 10 % (w/w), and HFD + P.RBE 10 % (w/w) respectively. Data are presented as mean ± SEM (n = 8). Significant differences are represented by: *p < 0.05; **p < 0.01 as compared to HFD diet group (one-way ANOVA with Dunnett's test as post-hoc).

protein levels. iNOS suppressors have shown to inhibit LPS-stimulated NO productions [45, 46]. Hence, suppressive effects of RBEs on NO production in LPS-stimulated J774A.1 macrophage cells were likely attribute to their ability to modulate LPS-stimulated overexpression of iNOS at gene and protein levels.

Among the different arrays of pro-inflammatory cytokines, TNF-α is of particular importance, acting as the potent key mediator of inflammatory responses by regulating the overproductions of other downstream pro-inflammatory chemokines and cytokines, such as IL-1α, IL-1β, and IL-6. Prolonged overproductions of these pro-inflammatory cytokines are closely associated with onset and progression of chronic diseases [47]. Hence, suppressions of pro-inflammatory cytokines remain pivotal to regulate adverse effects of chronic inflammation. The anti-inflammatory properties of RBE is likely attributed to the synergistic protective effect of its polyphenols, γ-oryzanol, and vitamins. RBE is likely to modulate overproduction of pro-inflammatory mediators through potent inhibition of pro-inflammatory nuclear factor kappa B (NF-κB) signaling pathways, and promote activations of mitogen activated protein kinase (MAPK) and antioxidant response element (ARE) [48, 49, 50, 51]. Regardless, extended investigations on the immunomodulatory mechanisms of these RBEs remain warranted.

3.4. Effects of RBE dietary supplementation on body weights, plasma lipid profiles, aortic lesions of Ldlr$^{-/-}$ *mice*

Having demonstrated the potent antioxidant and anti-inflammatory properties of RBE *in vitro*, ameliorative effects of RBE in modulating risk factors of atherosclerosis was further evaluated *in vivo* by using HFD-fed *Ldlr*$^{-/-}$ mice as atherosclerosis study models. No significant difference was observed in average body weights of different groups of *Ldlr*$^{-/-}$ mice throughout 12 weeks of animal experiment (Figure 9a). HFD induced dyslipidemia in *Ldlr*$^{-/-}$ mice as demonstrated through increments of total cholesterol and triglyceride at plasma levels. Dietary supplementations of R.RBE and P.RBE showed potent counteractivity by improving the plasma lipid profiles of *Ldlr*$^{-/-}$ mice. Plasma levels of total cholesterol (Figure 9b) and triglyceride (Figure 9c) of *Ldlr*$^{-/-}$ mice in R.RBE and P.RBE supplemented groups were significantly reduced ($p < 0.05$) from week 3 (R.RBE) and week 6 (P.RBE) onwards.

Plasma level of oxLDL/β2GPI, a novel pro-atherogenic biomarker was measured to evaluate the progression of atherosclerosis. A gradual increment in plasma level of oxLDL/β2GPI was observed in HFD mice group (Figure 9d). Although increment in plasma level of oxLDL/β2GPI was also seen in HFD + RBEs groups, the HFD-induced incremental effects of oxLDL/β2GPI at plasma levels were significantly suppressed (p <

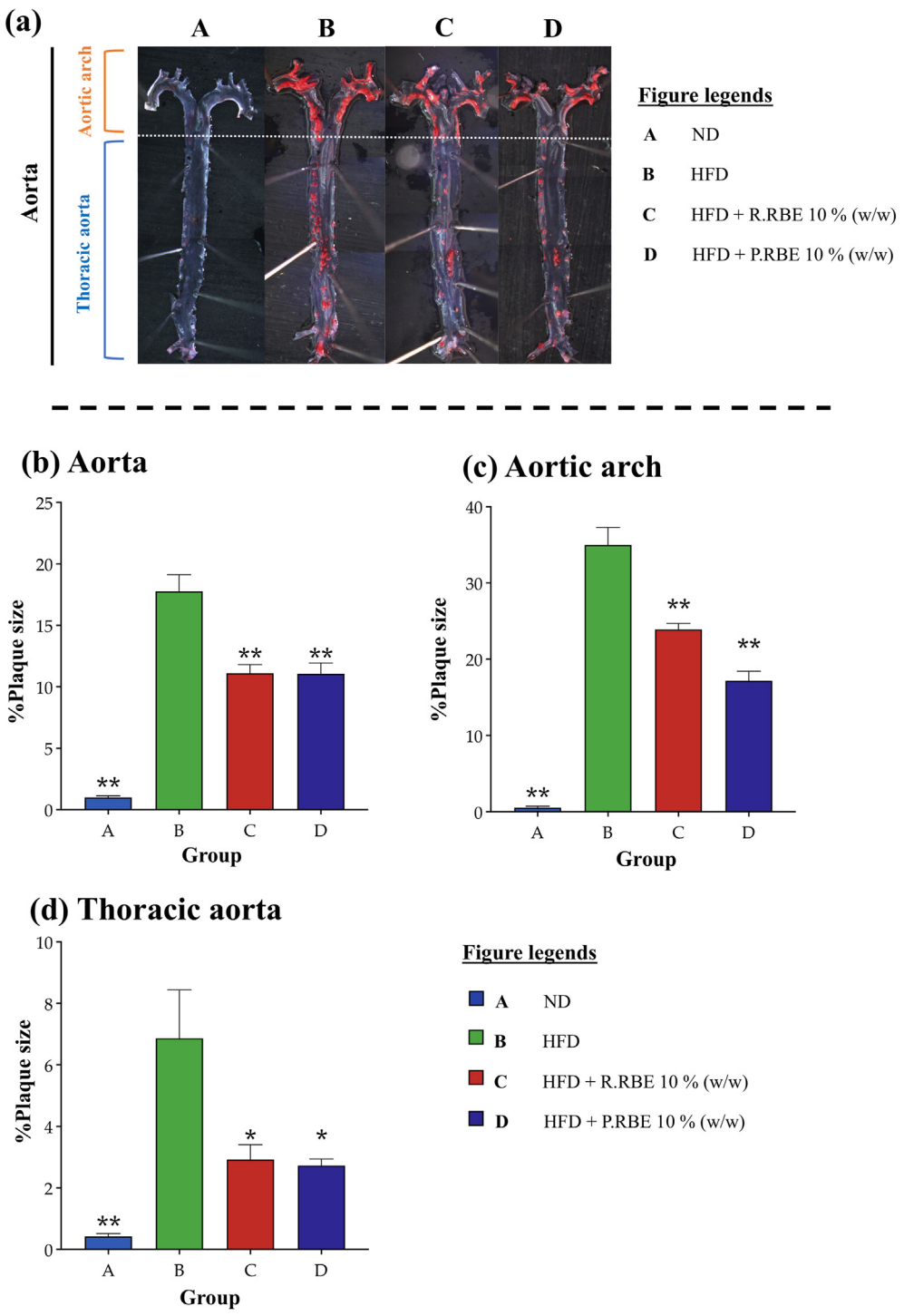

Figure 10. En face analyses of aorta atherosclerotic lesions. (a) Representative images of atherosclerotic plaques in aortas of *Ldlr*$^{-/-}$ mice fed with different diets. ORO stain was used to stain neutral lipids in atherosclerotic lesions. The sizes of atherosclerotic plaques were quantified en face and presented in % plaque size of total areas of (b) total vessel, (c) aortic arch, and (d) thoracic aorta respectively. Data are presented as mean ± SEM (n = 6). Significant differences are represented by: *p < 0.05; **p < 0.01 as compared to HFD group (one way ANOVA with Dunnett's test as post-hoc).

0.01) through dietary supplementations of RBEs from week 6 onwards (Figure 9d).

Aortas of *Ldlr*$^{-/-}$ mice were excised and en faced to evaluate the progression of atherosclerosis. ORO stains were used to stain neutral lipids in atherosclerotic lesions (Figure 10a). Twelve weeks of HFD feedings induced developments of severe atherosclerotic lesions in aortas of *Ldlr*$^{-/-}$ mice as compared to ND group. Dietary supplementations of R.RBE and P.RBE significantly reduced ($p < 0.01$) lipid depositions and sizes of atherosclerotic lesions in aortas of *Ldlr*$^{-/-}$ mice by 38% respectively (Figure 10b). Severe lipid depositions were observed mainly in the aortic arch of HFD group. Dietary supplementations of R.RBE and P.RBE significantly reduced ($p < 0.01$) lipid depositions in aortic arch by 32% and 51% respectively as compared to HFD group (Figure 10c). Atherosclerotic lesions in thoracic aorta regions of RBE supplemented groups were also significantly smaller ($p < 0.05$) than those in HFD group (Figure 10d).

The present study utilized *Ldlr*$^{-/-}$ mice lacking LDL receptor (LDLr) as an *in vivo* study model to evaluate the anti-atherogenic properties of RBE dietary supplementation. HFD feeding was administered to develop atherosclerotic phenotype in these mice. Due to defective LDLr, LDL metabolisms in these mice are impaired. These mice are known for expressing high circulatory levels of cholesterol and rapid development of atherosclerotic lesions [52]. Supplementations of rice bran and rice bran oil have demonstrated anti-atherogenic effects through their

antioxidant, anti-inflammatory and cholesterol-lowering properties in human subjects and rodents [14, 53, 54]. Though dietary supplementations of respective R.RBE and P.RBE as demonstrated in the present study significantly improved plasma lipid profile (reduced levels of total cholesterol and triglycerides) and decreased aortic plaque sizes of HFD-fed *Ldlr*$^{-/-}$ mice, the underlying hypolipidemic properties of both R.RBE and P.RBE in the context of this study remains warranted. Potent hypolipidemic properties of RBE (rice bran enzymatic extract) through enhanced fecal cholesterol disposition and alleviation of β-Hydroxy β-methylglutaryl-CoA (HMG-CoA) reductase-mediated liver steatosis reported by other research group may lend support to our findings [54].

The indissociable complexation of β2GPI and oxLDL into oxLDL/β2GPI is mediated through 7-ketocholesteryl-9-carboxynonanoate (oxLig-1), a specific ligand for β2GPI in oxLDL [33]. OxLDL/β2GPI complexes exhibit atherogenicity in the presence of anti-oxLDL/β2GPI autoantibodies. The uptake of these immunogenic complexes by macrophages accelerates the prevalence of foam cell formation and atherosclerosis progression [33, 55, 56]. Hence, circulatory plasma oxLDL/β2GPI complexes released from vulnerable and unstable plaque may represent a crucial biomarker for disease prognosis and risk assessment of atherosclerosis progression [57]. Dietary supplementations of R.RBE and P.RBE in the present study have significantly reduced the plasma levels of oxLDL/β2GPI in HFD group as compared to control group (HFD only). The antioxidant and hypolipidemic properties of R.RBE and P.RBE are likely the key attributes to such observation. The antioxidant capacity of RBE may attenuate inadvertent oxidative modifications of LDL into oxLDL while the hypolipidemic properties of RBE improved the lipid profiles of *Ldlr*$^{-/-}$ mice through significant reductions of plasma levels cholesterol and triglyceride.

3.5. Localizations of neutral lipids, oxLDL/β2GPI, macrophage infiltrations, and migrations of smooth muscle cells in atherosclerotic plaque

Frozen sections of aortic sinuses were used as anatomical landmarks to characterize the development and progression of atherosclerosis. The onset and progressive development of atherosclerotic lesion in aortic

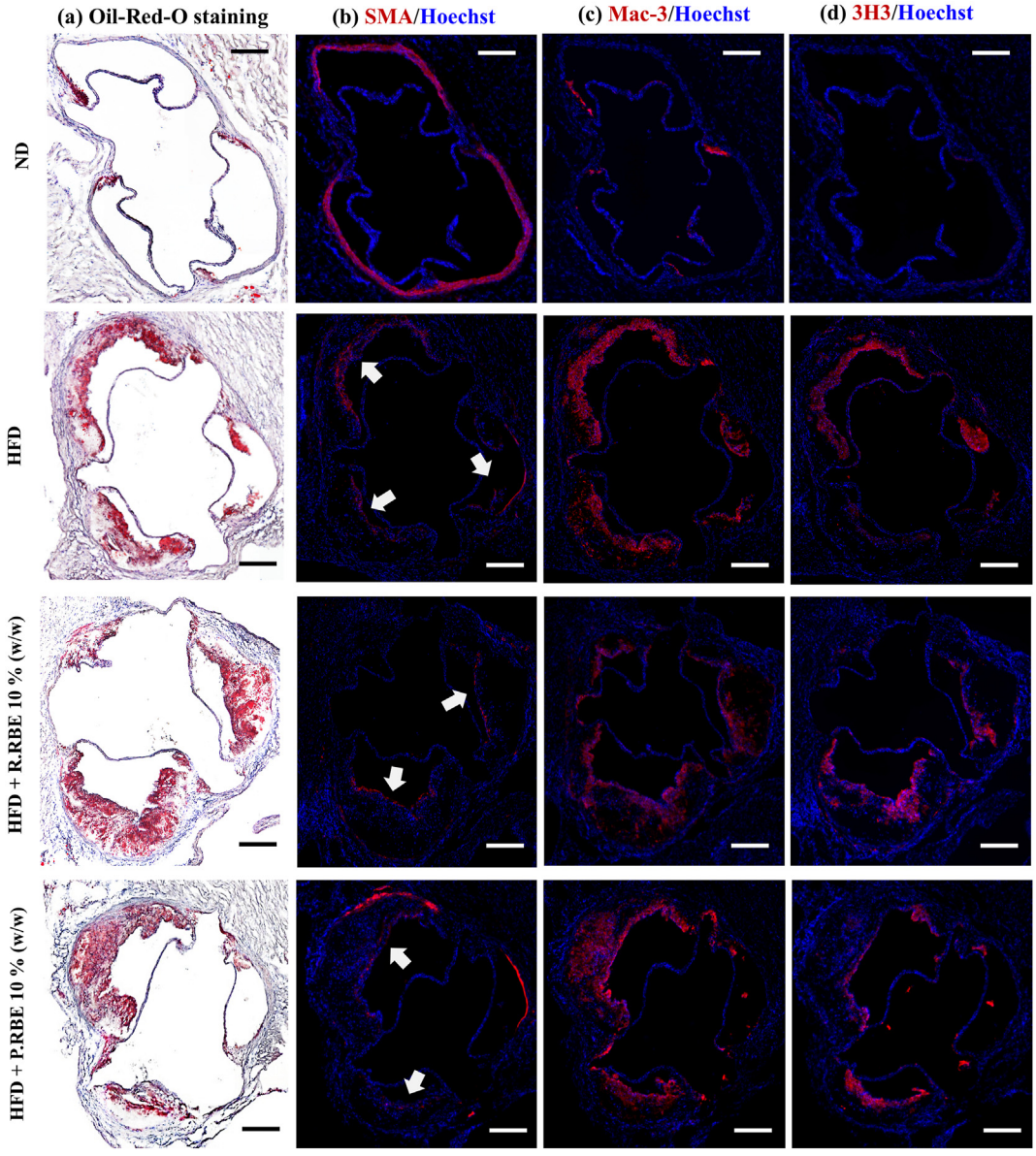

Figure 11. Characterizations of atherosclerotic lesions in aortic sinuses of *Ldlr*$^{-/-}$ mice. (a) Neutral lipids in atherosclerotic lesions were stained with ORO stain. Frozen sections of aortic sinuses were immunostained with antibodies against (b) α-smooth muscle actin of smooth muscle cells, (c) CD107b of activated macrophage, and (d) β2GPI complexed with oxLDL. Hoechst was used as counterstain for nuclei. White arrow insets show migrations of smooth muscle cells from vascular intima to media. Scale bar = 200 μm.

sinus are histologically characterized by accumulation of lipid deposit in lesion, migration of smooth muscle cells and macrophage infiltrations. Lesion developments were observed in aortic sinuses of HFD-fed groups, in regions where hydrophobic and neutral lipids in lesions were positively stained by ORO stain (Figure 11a). Migrations of smooth muscles cells from the media were also observed through positive staining of smooth muscle cells actin (indicated by white arrows) encapsulating the developed lesions in sectioned aortic sinuses of HFD-fed groups (Figure 11b). Co-localizations of macrophage-derived lipid laden foam cells (Figure 11c) and oxLDL/β2GPI complexes (Figure 11d) within atherosclerotic lesions were also observed through positive stainings of macrophages and β2GPI complexed with oxLDL in sectioned aortic sinuses of HFD-fed groups.

Present study has demonstrated the lipid accumulation, migration of vascular smooth muscle cell (VSMC), macrophage infiltration, and co-localizations of foam cells and oxLDL/β2GPI (uptake by macrophage) in atherosclerotic lesion through histological and immunohistochemical staining. These observations represent the pathological features of atherosclerotic plaque development. Early stage of atherosclerotic lesion begins with LDL retention in vessel wall and its subsequent oxidation into

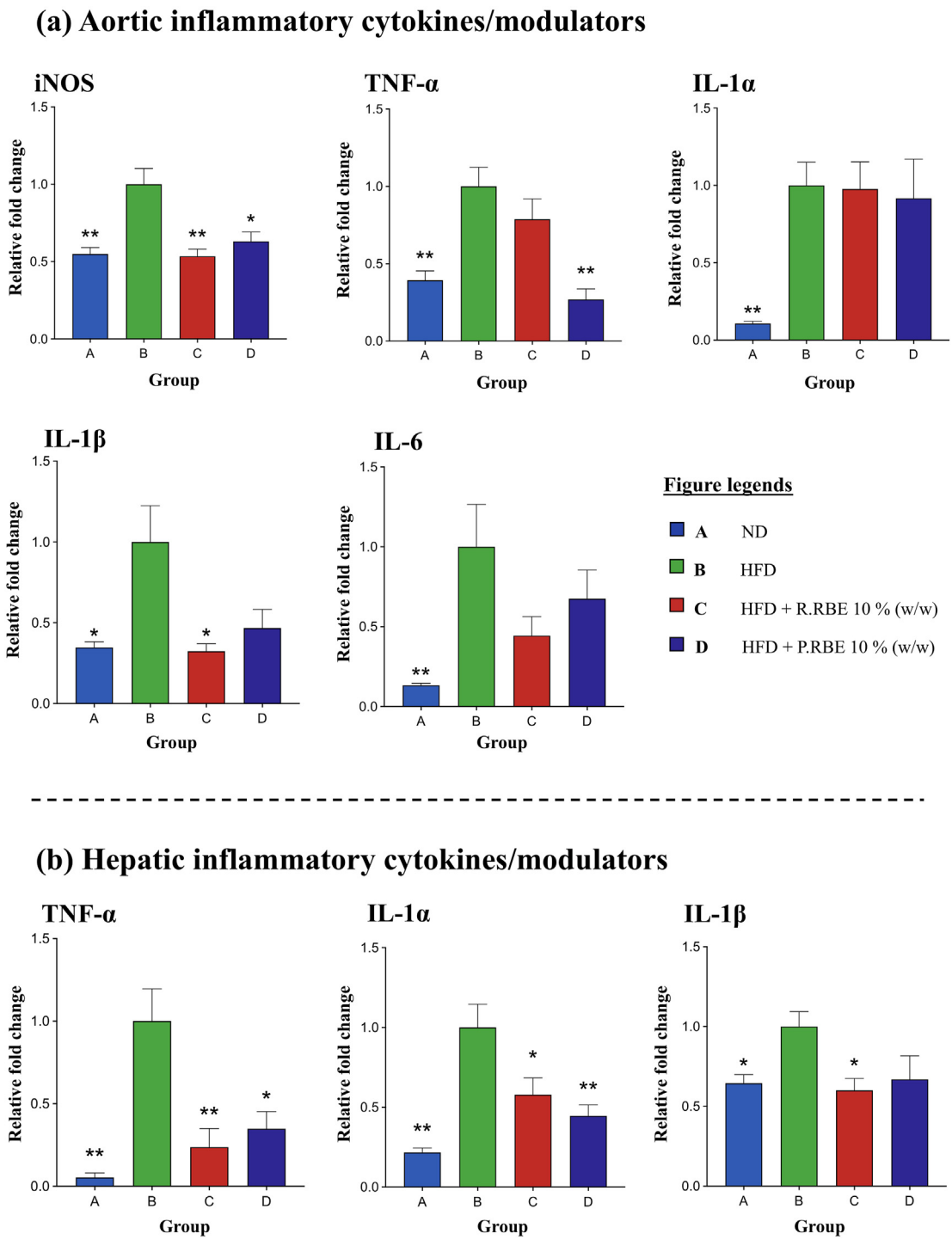

Figure 12. Effects of different diets on gene expressions of (a) aortic and (b) hepatic inflammatory cytokines/modulators. Expression levels of targeted genes were normalized against reference control gene (GADPH). Data are presented as means of fold changes of mRNA transcripts relative to HFD diet group ±SEM (n = 8). Significant differences are represented by: *p < 0.05; **p < 0.01 (one way ANOVA with Dunnett's analysis as post-hoc).

oxLDL promotes the recruitment, infiltration and activation of monocytes into macrophages. The uptake of LDL by macrophages escalates the formation of foam cells and progressively expand the size of lipid-rich necrotic core (consisting of extracellular lipid deposits from foam cells) in atheroma [58]. The migration of VSMC from media to intima exhibits biphasic effect. VSMC in early stage of atherosclerotic lesion mediates the uptake of LDL and monocyte infiltration into the arterial wall [59]. In advanced atherosclerotic lesion, VSMC-derived smooth muscle α-actin positive subtype presumably form thin fibrous cap over the lesion as a counteractive mechanism to stabilize the plaque from rupture [60].

3.6. Dietary supplementations of RBE downregulated gene expressions of aortic and hepatic inflammatory cytokines/modulators of $Ldlr^{-/-}$ mice

Gene expressions of aortic and hepatic inflammatory cytokines or modulators were assessed to evaluate potent anti-inflammatory properties of RBEs dietary supplementations in modulating inflammation-mediated atherosclerosis. Aortic gene expression levels of TNF-α, IL-1α, IL-1β, IL-6 and iNOS were measured to evaluate the ameliorative effects of RBEs dietary supplementations in modulation of localized inflammation in aorta. Aortic gene expression levels of iNOS, TNF-α, IL-1α, IL-1β, and IL-6 were significantly upregulated after 12 weeks of HFD feeding (Figure 12a). Dietary supplementations of R.RBE and P.RBE in HFD feeding significantly downregulated HFD-induced gene expressions of aortic iNOS by 46% ($p < 0.01$) and 37% ($p < 0.05$) respectively. P.RBE significantly reduced the gene expression of aortic TNF-α ($p < 0.01$) by 73% while R.RBE significantly decreased ($p < 0.05$) the gene expression of aortic IL-1β by 67%. Dietary supplementations of both RBEs did not have any significant effect on the gene expression levels of aortic IL-1α and IL-6 (Figure 12a).

In liver, 12 weeks of HFD feeding also upregulated the gene expression levels of TNF-α, IL-1α, and IL-1β (Figure 12b). Dietary supplementations of R.RBE and P.RBE in HFD-fed group significantly downregulated the gene expression of TNF-α by 76% ($p < 0.01$) and 65% ($p < 0.05$) respectively. Significant decrements in gene expression levels of hepatic IL-1α were also observed in HFD-fed group supplemented with R.RBE (by 44%; $p < 0.05$) and P.RBE (by 55%; $p < 0.01$) respectively. Dietary supplementation of R.RBE significantly reduced ($p < 0.01$) the gene expression of hepatic IL-1β (by 40%) to basal level in HFD-induced group.

High-grade local inflammation in atherosclerotic plaque is predominantly mediated by activated macrophages expressing pro-inflammatory biomarkers [61]. Pro-inflammatory cytokines such as TNF-α and IL-1 promote expression of adhesion molecules that stimulate recruitments of leucocytes and exacerbate the developmental process of atherosclerotic plaque by creating a microenvironment enriched with pro-inflammatory mediators [62]. The activation of iNOS in the presence of inflammatory stimuli mediates overproduction of NO and impairs endothelial functions [63]. The copious amount of NO derived from iNOS is highly reactive with superoxide ($O_2^{\cdot-}$), producing peroxynitrite that promotes oxidative stress and induces oxidation of LDL [44, 64]. Dietary supplementations of R.RBE and P.RBE have downregulated the expression levels of iNOS, TNF-α, and IL-1β. The anti-inflammatory properties of RBEs is likely attributed to their antioxidative properties through inhibition of inadvertent oxidative stress mediated by HFD and thus reducing the tendency of oxidative stress-mediated inflammatory responses. RBEs may also ameliorate inflammatory responses mediated by activated macrophages (M1 macrophages) localized in atherosclerotic plaques, as demonstrated in *in vitro* LPS-stimulated J774A.1 macrophage-like cell study model.

HFD-induced fatty liver disease is often associated with metabolic inflammation which promotes hepatic lipid accumulation and expressions of pro-inflammatory TNF-α, IL-1α, and IL-1β [65, 66]. Dietary supplementations of R.RBE and P.RBE in HFD-fed $Ldlr^{-/-}$ mice have downregulated the gene expression levels of hepatic TNF-α, IL-1α, and IL-1β. Antioxidative attributes of both RBEs may indirectly modulate the gene expressions of hepatic pro-inflammatory cytokines. Cholesterol-lowering effect of RBEs as demonstrated in this study may contribute to the attenuation of HFD-induced hepatic lipid accumulation. In addition, the antioxidative properties of RBEs may also alleviate ROS-induced lipid peroxidation and modulate TNF-α-induced liver damage through suppressions of pro-inflammatory cytokines [67].

4. Conclusion

Preliminary findings from this study have demonstrated the potent ameliorative effects of RBE in modulating risk factors associated with atherosclerosis. Although phytochemical profile of R.RBE appeared to be more superior than that of P.RBE, there was no distinctive difference between their bioactivities, particularly in *in vivo* study. Nonetheless, present study still highlights the potent ameliorative attributes of R.RBE and P.RBE in attenuating risk factors associated with atherosclerosis. These observations are likely attributed to the synergistic actions of bioactive constituents in both R.RBE and P.RBE. However, it is still worth to note that additional works remain warranted to further elucidate the precise underlying ameliorative attributes of RBE in alleviation of atherosclerosis. In addition, present study remained restricted by limited knowledge on bioactivity and bioavailability of individual phytochemical in RBEs. Hence, future studies along the lines of metabonomics will offer insights into underlying multiparametric mechanisms of RBEs in amelioration of atherosclerosis. With further investigations, RBE could be potentially utilized as dietary supplement not only for management of atherosclerosis but also for general health and wellness in near future.

Declarations

Author contribution statement

Xian Wen Tan: Conceived and designed the experiments; Performed the experiments; Analyzed and interpreted the data; Contributed reagents, materials, analysis tools or data; Wrote the paper.

Kazuko Kobayashi, Lianhua Shen, Junko Inagaki, Masahiro Ide, Siaw San Hwang: Conceived and designed the experiments; Analyzed and interpreted the data; Contributed reagents, materials, analysis tools or data.

Eiji Matsuura: Conceived and designed the experiments; Analyzed and interpreted the data; Contributed reagents, materials, analysis tools or data; Wrote the paper.

Funding statement

This research was supported in part by a grant from the Ministry of Education, Culture, Sports, Science and Technology of Japan; KAKEN (Japan Society for the Promotion of Science [JSPS]), Grant Number: 26253036.

Data availability statement

The data will be deposited into Okayama University library repository and made publicly available once the manuscript receives official acceptance from the journal publisher.

Declaration of interests statement

The authors declare no conflict of interest.

Additional information

Supplementary content related to this article has been published online at https://doi.org/10.1016/j.heliyon.2020.e05743.

Acknowledgements

The authors acknowledge Mr. Haruo Kobayashi (Okayama Prefecture University, Okayama, Japan), Mr. Shogo Namba (Red Rice Company, Okayama, Japan), Mr. Junichi Furuichi (Shin-eibusan Co. Ltd, Kagoshima, Japan) and Mr. Kazumasa Seno (Yakage City Government Office, Okayama, Japan) for acquisitions of rice samples; Dr. Hirotsugu Kobuchi (Okayama University, Okayama, Japan) and Ms. Kyoko Tarora (Okayama Agriculture Development Institute, Okayama, Japan) for technical advices; Central Research Laboratory of Okayama University Medical School for access to research instruments (FlexStation 3 microplate reader, StepOnePlus Real-Time PCR system, TL-100 ultracentrifuge machine, Olympus SZX12 stereoscopic microscope equipped with Olympus DP72 charged-coupled device, and Keyence BZ-X700 All-in-one fluorescence microscope).

References

[1] B.H. Toh, T. Kyaw, P. Tipping, A. Bobik, Atherosclerosis, in: N.R. Rose, I.R.B.T. T.A.D., Fifth E. Mackay (Eds.), Autoimmune Dis, fifth ed., Academic Press, Boston, 2013, pp. 1049–1066.
[2] A.D. Mooradian, Dyslipidemia in type 2 diabetes mellitus, Nat. Clin. Pract. Endocrinol. Metabol. 5 (2009) 150–159.
[3] W. Palinski, M.E. Rosenfeld, S. Yla-Herttuala, G.C. Gurtner, S.S. Socher, S.W. Butler, S. Parthasarathy, T.E. Carew, D. Steinberg, J.L. Witztum, Low density lipoprotein undergoes oxidative modification in vivo, Proc. Natl. Acad. Sci. U. S. A. 86 (1989) 1372–1376.
[4] P. Libby, Inflammation in atherosclerosis, Nature 420 (2002) 868–874.
[5] G.K. Hansson, Mechanisms of disease: inflammation, atherosclerosis, and coronary artery disease, N. Engl. J. Med. 352 (2005) 1685–1695.
[6] G. Paliyath, M. Bakovic, K. Shetty, Functional Foods, Nutraceuticals, and Degenerative Disease Prevention, Wiley, 2011.
[7] B. Poljšak, R. Fink, The protective role of antioxidants in the defence against ROS/RNS-mediated environmental pollution, Oxid. Med. Cell. Longev. 2014 (2014) 671539.
[8] V. Van Hoed, G. Depaemelaere, J.V. Ayala, P. Santiwattana, R. Verhé, W. De Greyt, Influence of chemical refining on the major and minor components of rice bran oil, JAOCS, J. Am. Oil Chem. Soc. 83 (2006) 315–321.
[9] A. Chakraverty, R. Paul Singh, Postharvest Technology and Food Process Engineering, CRC Press, 2016.
[10] A. Sirikul, A. Moongngarm, P. Khaengkhan, Comparison of proximate composition, bioactive compounds and antioxidant activity of rice bran and defatted rice bran from organic rice and conventional rice, Asian J. Food Agro-Industry 2 (2009) 731–743.
[11] T.A. Wilson, H.M. Idreis, C.M. Taylor, R.J. Nicolosi, Whole fat rice bran reduces the development of early aortic atherosclerosis in hypercholesterolemic hamsters compared with wheat bran, Nutr. Res. 22 (2002) 1319–1332.
[12] L.M. Ausman, N. Rong, R.J. Nicolosi, Hypocholesterolemic effect of physically refined rice bran oil: studies of cholesterol metabolism and early atherosclerosis in hypercholesterolemic hamsters, J. Nutr. Biochem. 16 (2005) 521–529.
[13] M.L. Justo, M. Candiracci, A.P. Dantas, M.A. de Sotomayor, J. Parrado, E. Vila, M.D. Herrera, R. Rodriguez-Rodriguez, Rice bran enzymatic extract restores endothelial function and vascular contractility in obese rats by reducing vascular inflammation and oxidative stress, J. Nutr. Biochem. 24 (2013) 1453–1461.
[14] C.K. Pushpan, V. Shalini, G. Sindhu, P. Rathnam, A. Jayalekshmy, A. Helen, Attenuation of atherosclerotic complications by modulating inflammatory responses in hypercholesterolemic rats with dietary Njavara rice bran oil, Biomed. Pharmacother. 83 (2016) 1387–1397.
[15] P.K. Chithra, A. Jayalekshmy, A. Helen, Petroleum ether extract of Njavara rice (Oryza sativa) bran upregulates the JAK2-STAT3-mediated anti-inflammatory profile in macrophages and aortic endothelial cells promoting regression of atherosclerosis, Biochem. Cell. Biol. 95 (2017) 652–662.
[16] M.H. Hong Bang, T. Van Riep, N.T. Thinh, L.E. Huu Song, T.T. Dung, L.E. Van Truong, L.E. Van Don, K.Y. Thai Doan, P. Deyu, M. Shaheen, M. Ghoneum, Arabinoxylan rice bran (MGN-3) enhances the effects of interventional therapies for the treatment of hepatocellular carcinoma: a three-year randomized clinical trial, Anticancer Res. 30 (2010) 5145–5152. http://ar.iiarjournals.org/content/30/12/5145.abstract.
[17] A.J. Henderson, C.A. Ollila, A. Kumar, E.C. Borresen, K. Raina, R. Agarwal, E.P. Ryan, Chemopreventive properties of dietary rice bran: current status and future prospects, Adv. Nutr. 3 (2012) 643–653.
[18] J.S.L. De Munter, F.B. Hu, D. Spiegelman, M. Franz, R.M. Van Dam, Whole grain, bran, and germ intake and risk of type 2 diabetes: a prospective cohort study and systematic review, PLoS Med. 4 (2007) 1385–1395.
[19] M.M. Most, R. Tulley, S. Morales, M. Lefevre, Rice bran oil, not fiber, lowers cholesterol in humans, Am. J. Clin. Nutr. 81 (2005) 64–68.
[20] N. Quan, K. Kobayashi, Y. Matsunami, M. Ide, M. Makarova, L. Shen, S. Ohno, Y. Zheng, H. Kobayashi, L.R. Lopez, E. Matsuura, Persimmon (Diospyros kaki thunb 'saijo') peel improved dyslipidemia and its related production of atherogenic autoantigen complexes in low- density lipoprotein receptor-deficient mice, Open Nutr. J. 6 (2012) 12–20.
[21] E.T. Champagne, D.F. Wood, B.O. Juliano, D.B. Bechtel, Chapter 4: the rice grain and its gross composition, in: RICE Chem. Technol., 2004, pp. 77–107.
[22] X.W. Tan, M. Bhave, A.Y.Y. Fong, E. Matsuura, K. Kobayashi, L.H. Shen, S.S. Hwang, Cytoprotective and cytotoxic effects of rice bran extracts in rat H9c2(2-1) cardiomyocytes, Oxid. Med. Cell. Longev. 2016 (2016).
[23] V.L. Singleton, J.A. Rossi, Colorimetry of total phenolics with phosphomolybdic-phosphotungstic acid reagents, Am. J. Enol. Vitic. 16 (1965) 144–158. http://www.ajevonline.org/content/16/3/144.abstract.
[24] Z. Jia, M. Tang, J. Wu, The determination of flavonoid contents in mulberry and their scavenging effects on superoxide radicals, Food Chem. 64 (1999) 555–559.
[25] T.J. Herald, P. Gadgil, M. Tilley, High-throughput micro plate assays for screening flavonoid content and DPPH-scavenging activity in sorghum bran and flour, J. Sci. Food Agric. 92 (2012) 2326–2331.
[26] M.M. Giusti, R.E. Wrolstad, Characterization and measurement of anthocyanins by UV-visible spectroscopy, Curr. Protoc. Food Anal. Chem. (2001) F1.2.1–F1.2.13.
[27] T.J. Herald, P. Gadgil, R. Perumal, S.R. Bean, J.D. Wilson, High-throughput micro-plate HCl-vanillin assay for screening tannin content in sorghum grain, J. Sci. Food Agric. 94 (2014) 2133–2136.
[28] R. Bucci, A.D. Magrì, A.L. Magrì, F. Marini, Comparison of three spectrophotometric methods for the determination of γ-oryzanol in rice bran oil, Anal. Bioanal. Chem. 375 (2003) 1254–1259.
[29] N.J. Miller, C. Rice-Evans, M.J. Davies, V. Gopinathan, A. Milner, A novel method for measuring antioxidant capacity and its application to monitoring the antioxidant status in premature neonates, Clin. Sci. 84 (1993) 407–412.
[30] C.D. Fernando, P. Soysa, Optimized enzymatic colorimetric assay for determination of hydrogen peroxide (H2O2) scavenging activity of plant extracts, MethodsX 2 (2015) 283–291.
[31] L.C. Green, D.A. Wagner, J. Glogowski, P.L. Skipper, J.S. Wishnok, S.R. Tannenbaum, Analysis of nitrate, nitrite, and [15N]nitrate in biological fluids, Anal. Biochem. 126 (1982) 131–138.
[32] M. Jesús Andrés-Manzano, V. Andrés, B. Dorado, Oil red O and hematoxylin and eosin staining for quantification of atherosclerosis burden in mouse aorta and aortic root, Methods Mol. Biol. (2015) 85–99.
[33] K. Kobayashi, E. Matsuura, Q. Liu, J.I. Furukawa, K. Kaihara, J. Inagaki, T. Atsumi, N. Sakairi, T. Yasuda, D.R. Voelker, T. Koike, A specific ligand for β2-glycoprotein I mediates autoantibody-dependent uptake of oxidized low density lipoprotein by macrophages, J. Lipid Res. 42 (2001) 697–709.
[34] X.W. Tan, F. Takenaka, H. Takekawa, E. Mastuura, Rapid and specific detection of oxidized LDL/β2GPI complexes via facile lateral flow immunoassay, Heliyon 6 (2020), e04114.
[35] P.R. Ames, A. Ortiz-Cadenas, I. Garcia-De La Torre, A. Nava, A. Oregon-Miranda, J.R. Batuca, K. Kojima, L.R. Lopez, E. Matsuura, Rosuvastatin treatment is associated with a decrease of serum oxidised low-density lipoprotein/beta2-glycoprotein i complex concentration in type 2 diabetes, Br. J. Diabetes Vasc. Dis. 10 (2010) 292–299.
[36] L. Shen, Y. Matsunami, N. Quan, K. Kobayashi, E. Matsuura, K. Oguma, In vivo oxidation, platelet activation and simultaneous occurrence of natural immunity in atherosclerosis-prone mice, Isr. Med. Assoc. J. 13 (2011) 278–283.
[37] E.C. Borresen, E.P. Ryan, Rice bran. A food ingredient with global public health opportunities, in: R.R. Watson, V.R. Preedy, S.B. TW, D. P, H. Zibadi (Eds.), Wheat Rice Dis. Prev. Heal., Academic Press, San Diego, 2014, pp. 301–310.
[38] T. Hussain, B. Tan, Y. Yin, F. Blachier, M.C.B. Tossou, N. Rahu, Oxidative stress and inflammation: what polyphenols can do for us? Oxid. Med. Cell. Longev. 2016 (2016) 7432797.
[39] R. Tsao, Chemistry and biochemistry of dietary polyphenols, Nutrients 2 (2010) 1231–1246.
[40] C.A. Rice-Evans, N.J. Miller, G. Paganga, Structure-antioxidant activity relationships of flavonoids and phenolic acids, Free Radic. Biol. Med. 20 (1996) 933–956.
[41] K.J. Moore, I. Tabas, Macrophages in the pathogenesis of atherosclerosis, Cell 145 (2011) 341–355.
[42] N. Leyva-López, E.P. Gutierrez-Grijalva, D.L. Ambriz-Perez, J. Basilio Heredia, Flavonoids as cytokine modulators: a possible therapy for inflammation-related diseases, Int. J. Mol. Sci. 17 (2016) 921.
[43] J.W. Coleman, Nitric oxide in immunity and inflammation, Int. Immunopharm. 1 (2001) 1397–1406.
[44] M. Gliozzi, M. Scicchitano, F. Bosco, V. Musolino, C. Carresi, F. Scarano, J. Maiuolo, S. Nucera, A. Maretta, S. Paone, R. Mollace, S. Ruga, M.C. Zito, R. Macrì, F. Oppedisano, E. Palma, D. Salvemini, C. Muscoli, V. Mollace, Modulation of nitric oxide synthases by oxidized LDLs: role in vascular inflammation and atherosclerosis development, Int. J. Mol. Sci. 20 (2019) 3294.
[45] S.K. Sandur, H. Ichikawa, G. Sethi, S.A. Kwang, B.B. Aggarwal, Plumbagin (5-hydroxy-2-methyl-1,4-naphthoquinone) suppresses NF-κB activation and NF-κB-regulated gene products through modulation of p65 and IκBα kinase activation, leading to potentiation of apoptosis induced by cytokine and chemotherapeutic agents, J. Biol. Chem. 281 (2006) 17023–17033.
[46] Y.W. Cheng, C.Y. Chang, K.L. Lin, C.M. Hu, C.H. Lin, J.J. Kang, Shikonin derivatives inhibited LPS-induced NOS in RAW 264.7 cells via downregulation of MAPK/NF-κB signaling, J. Ethnopharmacol. 120 (2008) 264–271.
[47] A. Rajput, C.F. Ware, Tumor necrosis factor signaling pathways, in: R.A. Bradshaw, P.D.B. T.E, C.B. Stahl (Eds.), Encycl. Cell Biol., Academic Press, Waltham, 2015, pp. 353–363.
[48] C. Santangelo, R. Varì, B. Scazzocchio, R. Di Benedetto, C. Filesi, R. Masella, Polyphenols, intracellular signalling and inflammation, Ann. Ist. Super Sanita 43 (2007) 394–405.

[49] G.C. Yen, Y.C. Chen, W.T. Chang, C.L. Hsu, Effects of polyphenolic compounds on tumor necrosis factor-α (TNF-α)-induced changes of adipokines and oxidative stress in 3T3-L1 adipocytes, J. Agric. Food Chem. 59 (2011) 546–551.
[50] A. Mastinu, S.A. Bonini, W. Rungratanawanich, F. Aria, M. Marziano, G. Maccarinelli, G. Abate, M. Premoli, M. Memo, D. Uberti, Gamma-oryzanol prevents LPS-induced brain inflammation and cognitive impairment in adult mice, Nutrients 11 (2019) 728.
[51] V. Shalini, C.K. Pushpan, G. S, A. J, A. H, Tricin, flavonoid from Njavara reduces inflammatory responses in hPBMCs by modulating the p38MAPK and PI3K/Akt pathways and prevents inflammation associated endothelial dysfunction in HUVECs, Immunobiology 221 (2016) 137–144.
[52] S. Ishibashi, J. Herz, N. Maeda, J.L. Goldstein, M.S. Brown, The two-receptor model of lipoprotein clearance: tests of the hypothesis in "knockout" mice lacking the low density lipoprotein receptor, apolipoprotein E, or both proteins, Proc. Natl. Acad. Sci. U. S. A. 91 (1994) 4431–4435.
[53] M. Friedman, Rice brans, rice bran oils, and rice hulls: composition, food and industrial uses, and bioactivities in humans, animals, and cells, J. Agric. Food Chem. 61 (2013) 10626–10641.
[54] C. Perez-Ternero, C. Claro, J. Parrado, M.D. Herrera, M. Alvarez de Sotomayor, Rice bran enzymatic extract reduces atherosclerotic plaque development and steatosis in high-fat fed ApoE−/− mice, Nutrition 37 (2017) 22–29.
[55] K. Kobayashi, K. Tada, H. Itabe, T. Ueno, P.H. Liu, A. Tsutsumi, M. Kuwana, T. Yasuda, Y. Shoenfeld, P.G. De Groot, E. Matsuura, Distinguished effects of antiphospholipid antibodies and anti-oxidized LDL antibodies on oxidized LDL uptake by macrophages, Lupus 16 (2007) 929–938.
[56] T. Kajiwara, T. Yasuda, E. Matsuura, Intracellular trafficking of β2-glycoprotein I complexes with lipid vesicles in macrophages: implications on the development of antiphospholipid syndrome, J. Autoimmun. 29 (2007) 164–173.
[57] E. Matsuura, K. Kobayashi, M. Tabuchi, L.R. Lopez, Oxidative modification of low-density lipoprotein and immune regulation of atherosclerosis, Prog. Lipid Res. 45 (2006) 466–486.
[58] R.B. Singh, S.A. Mengi, Y.J. Xu, A.S. Arneja, N.S. Dhalla, Pathogenesis of atherosclerosis: a multifactorial process, Exp. Clin. Cardiol. 7 (2002) 40–53.
[59] A.C. Doran, N. Meller, C.A. McNamara, Role of smooth muscle cells in the initiation and early progression of atherosclerosis, Arterioscler, Thromb. Vasc. Biol. 28 (2008) 812–819.
[60] R. Virmani, F.D. Kolodgie, A.P. Burke, A. Farb, S.M. Schwartz, Lessons from sudden coronary death: a comprehensive morphological classification scheme for atherosclerotic lesions, Arterioscler. Thromb. Vasc. Biol. 20 (2000) 1262–1275.
[61] Y.V. Bobryshev, E.A. Ivanova, D.A. Chistiakov, N.G. Nikiforov, A.N. Orekhov, Macrophages and their role in atherosclerosis: pathophysiology and transcriptome analysis, BioMed Res. Int. 2016 (2016) 9582430.
[62] D.P. Ramji, T.S. Davies, Cytokines in atherosclerosis: key players in all stages of disease and promising therapeutic targets, Cytokine Growth Factor Rev. 26 (2015) 673–685.
[63] U. Förstermann, E.I. Closs, J.S. Pollock, M. Nakane, P. Schwarz, I. Gath, H. Kleinert, Nitric oxide synthase isozymes characterization, purification, molecular cloning, and functions, Hypertension 23 (1994) 1121–1131.
[64] L.D.K. Buttery, D.R. Springall, A.H. Chester, T.J. Evans, N. Standfield, D.V. Parums, M.H. Yacoub, J.M. Polak, Inducible nitric oxide synthase is present within human atherosclerotic lesions and promotes the formation and activity of peroxynitrite, Lab. Invest. 75 (1996) 77–85.
[65] A.R. Moschen, C. Molnar, S. Geiger, I. Graziadei, C.F. Ebenbichler, H. Weiss, S. Kaser, A. Kaser, H. Tilg, Anti-inflammatory effects of excessive weight loss: potent suppression of adipose interleukin 6 and tumour necrosis factor a expression, Gut 59 (2010) 1259–1264.
[66] L. Niederreiter, H. Tilg, Cytokines and fatty liver diseases, Liver Res. 2 (2018) 14–20.
[67] G. Chen, Y. Ni, N. Nagata, L. Xu, T. Ota, Micronutrient antioxidants and nonalcoholic fatty liver disease, Int. J. Mol. Sci. 17 (2016).